NUREG/CR-3307
Vol. 3
PNL-4705-3

Reactor Safety Research Programs

Quarterly Report
July-September 1983

Prepared by S. K. Edler, Ed.

Pacific Northwest Laboratory
Operated by
Battelle Memorial Institute

Prepared for
U.S. Nuclear Regulatory
Commission

GPO Printed copy price: $4.50

NUREG/CR-3307
Vol. 3
PNL-4705-3
R3, 4, 5, GS

Reactor Safety Research Programs

Quarterly Report
July-September 1983

Manuscript Completed: March 1984
Date Published: April 1984

Prepared by
S. K. Edler, Ed.

Pacific Northwest Laboratory
P.O. Box 999
Richland, WA 99352

Prepared for
Division of Accident Evaluation
Division of Engineering Technology
Office of Nuclear Regulatory Research
U.S. Nuclear Regulatory Commission
Washington, DC 20555
NRC FINs: B2101, B2088, B2289, B2043, B2452, B2383, B2449, B2084, B2456, B2864, B2372, B2455, B2041, B2277, B2097

ABSTRACT

This document summarizes work performed by Pacific Northwest Laboratory from July 1 through September 30, 1983, for the Division of Accident Evaluation and the Division of Engineering Technology, U.S. Nuclear Regulatory Commission. Evaluations of nondestructive examination (NDE) techniques and instrumentation include demonstrating the feasibility of determining the strength of structural graphite, evaluating the feasibility of detecting and analyzing flaw growth in reactor pressure boundary systems, and examining NDE reliability and probabilistic fracture mechanics. Accelerated pellet-cladding interaction modeling is being conducted to predict the probability of fuel rod failure under normal operating conditions. Experimental data and analytical models are being provided to aid in decision making regarding pipe-to-pipe impacts following postulated breaks in high-energy fluid system piping. Experimental data and validated models are being used to determine a method for evaluating the acceptance of welded or weld-repaired stainless steel piping. Thermal-hydraulic models are being developed to provide better digital codes to compute the behavior of full-scale reactor systems under postulated accident conditions. High-temperature materials property tests are being conducted to provide data on severe core damage fuel behavior. Severe fuel damage accident tests are being conducted at the NRU reactor, Chalk River, Canada; and an instrumented fuel assembly irradiation program is being performed at Halden, Norway. Fuel assemblies and analytical support are being provided for experimental programs at other facilities, including the Super Sara Test Program, Ispra, Italy, and experimental programs at the Power Burst Facility, Idaho National Engineering Laboratory, Idaho Falls, Idaho.

CONTENTS

FIGURES

COBRA Applications

TABLES

Integration of Nondestructive Examination Reliability and Fracture Mechanics

Experimental Support and Development of Single-Rod Fuel Codes

Accelerated Pellet-Cladding Interaction Modeling

Pipe-to-Pipe Impact

GRAPHITE NONDESTRUCTIVE TESTING (NDT) RESEARCH[a]

W. C. Morgan, Project Manager
J. M. Prince, Project Manager

D. K. Lemon
D. L. Lessor

SUMMARY

Technical progress and areas where additional work needs to be done are briefly discussed below.

INTRODUCTION

The objective of the Graphite NDT Research Program at Pacific Northwest Laboratory (PNL) was to demonstrate the feasibility of using NDT techniques for in-service monitoring of structural graphite strength in a high-temperature gas-cooled reactor (HTGR). During the course of the program, the following tasks were completed:

- The feasibility of monitoring strength changes due to oxidation of HTGR core support post graphites was proven by measuring ultrasonic velocities.
- The nonfeasibility of monitoring strength changes in oxidized PGX (core support block) material from ultrasonic velocity measurements was determined.
- The feasibility of using eddy-current techniques for obtaining near-surface oxidation profiles in PGX graphite was proven.
- A computerized algorithm was developed for analysis of data from sweep-frequency eddy-current measurements.
- The feasibility of obtaining oxidation profiles to greater depths than possible by eddy-current techniques was established using multifrequency ultrasonic backscattering techniques.

The scope of work for this project during FY 1983 was to:

- Modify the eddy-current probe design and obtain calibration constants to permit measurement of oxidation profiles in prototypic HTGR core support post graphite.
- Continue development of ultrasonic backscattering techniques for evaluation of in-depth oxidation profiles in HTGR core support components.

TECHNICAL PROGRESS

Technical progress during the first two quarters of FY 1983 included:

- Completed interfacing sweep-frequency eddy-current instrument[b] with an HP9826, programmed to act as the system controller and data logger.

(a) FIN: B2101-3; NRC Contact: R. B. Foulds.
(b) The existing field-portable sweep-frequency eddy-current instrument was designed and built under a related U.S. Department of Energy (DOE)-funded program.

- Completed fabrication and preliminary evaluation of two plano-concave transducers designed to obtain backscattering data over a wide range of graphite densities by operating in a tone-burst mode over a wide frequency range (0.5 to 1.25 MHz).
- Established a cooperative program with Oak Ridge National Laboratory to field test the portable sweep-frequency eddy-current instrument.
- Determined that the compressive strength of unoxidized PGX graphite is more variable than generally assumed.
- Determined that the average oxidation rates of individual logs of PGX graphite can vary by more than an order of magnitude.

Work on this program was stopped on April 23, 1983, when PNL learned that the anticipated funding would not be forthcoming.

The following publications were presented at the 16th Biennial Conference on Carbon, July 18-22, 1983, University of California at San Diego, San Diego, California:

- W. C. Morgan. "Disparate Changes in Physical Properties of Graphite."
- J. M. Prince and D. L. Lessor. "Computer-Controlled Sweep-Frequency Eddy-Current Instrument for Obtaining Electrical Conductivity Versus Depth Data on Oxidized Graphite."
- W. C. Morgan and J. M. Prince. "Relationships Between Strength, Electrical Conductivity, and Density of Oxidized PGX Graphite."

FUTURE WORK

The following work is currently not funded but needs to be done to complete the project:

- Demonstrate the feasibility of obtaining oxidation/strength measurements in situ.
- Complete the study of PGX variability as it relates to reliability of the sweep-frequency eddy-current technique.
- Establish optimum design parameters for monitoring oxidation depth profiles using multifrequency ultrasonic backscattering techniques.
- Demonstrate the feasibility of obtaining oxidation depth profiles in situ from ultrasonic backscattering measurements.

ACOUSTIC EMISSION/FLAW RELATIONSHIP FOR IN-SERVICE MONITORING OF NUCLEAR PRESSURE VESSELS(a)

P. H. Hutton, Project Manager
R. J. Kurtz, Assistant Project Manager

SUMMARY

The ZB-1 intermediate-scale vessel test at Mannheim, West Germany, was completed. Unanticipated cracking in a fabrication weld and at nozzle penetrations as well as crack growth in machined flaws was detected by acoustic emission (AE). Test results are being compiled for a topical report. AE monitoring of hot functional testing at the Watts Bar 1 reactor was completed. It was demonstrated that the problem of coolant flow noise interference with AE detection can be overcome. The fabrication of a compact AE system to monitor pipe weld areas is 90% complete.

INTRODUCTION

The purpose of this Pacific Northwest Laboratory (PNL) program is to provide an experimental evaluation of the feasibility of detecting and analyzing flaw growth in reactor pressure boundaries on a continuous basis using AE. Type A533B, Class 1 pressure vessel steel, and SA351-CF-8A cast stainless, Type 304 wrought, and A106 ferritic piping steels are being used in experimental testing. Objectives of this program are to:

- develop a method to identify crack growth AE signals in the presence of other acoustic signals
- develop a relationship to estimate flaw significance from AE data
- develop an instrument system to implement these techniques
- demonstrate the total concept off-reactor and on-reactor.

TECHNICAL PROGRESS

Progress relative to the objectives stated above is described in the following sections on off-reactor vessel test, reactor monitoring, pipe monitoring system, and reports.

OFF-REACTOR VESSEL TEST

The last six steps of the test plan for the ZB-1 vessel test at Mannheim, West Germany, were completed:

- Step 8 - 2000 pressure cycles (100 to 250 bar)
- Step 9 - 4000 pressure cycles (150 to 250 bar)
- Step 10 - hydrostatic test to 290 bar at 70°C
- Step 11 - 2000 pressure cycles (100 to 250 bar)
- Step 12 - 4000 pressure cycles (150 to 250 bar)
- Step 13 - hydrostatic test to 350 bar at 70°C.

(a) FIN: B2088; NRC Contact: J. Muscara.

The test proceeded smoothly until Cycle 1340 in Step 11. At that point, a leak developed at the base of a blanked nozzle on the vessel. The nozzle was inspected, and it was found that the leak was generated by crack growth in the vessel wall projecting radially from the bore of the nozzle penetration. The inspection also showed that various stages of cracking were in progress in the other seven similar nozzles. The decision was made to repair the leaking nozzle, go directly to the Step 13 hydrostatic test to 340 bar, and terminate the testing at that point. Before the Step 13 hydrostatic test, five German inspection organizations attempted to characterize the various flaws using normal in-service inspection (ISI) methods. In addition, samples were drilled at four locations on the KSO7 insert replacement weld to further characterize the cracking. These samples indicated that the cracks ranged from about 15 to 42 mm deep.

During Step 11, the data rate increased dramatically and most of the data appeared to originate from the KSO7 insert replacement weld area. At the end of Step 9 (the previous cyclic load step), the data rate was about 30 events per load cycle; by Cycle 1340 in Step 11, the rate had increased to 600 to 800 events per load cycle. Load position information developed from the 70°C testing suggests that a significant portion of the extremely high data rate was produced by oxide cracking. Such cracking could arise from oxide bonded to the inside metal surfaces or from loose oxide in the inside crack openings.

Figures 1 and 2 show the distribution of AE data relative to load position for Flaw B in Steps 5 and 6, indicating a pronounced concentration around the peak load position (75). Observation of the current data on an oscilloscope revealed that a large portion of the total data was occurring about halfway down the decreasing load curve, suggesting that oxide particles trapped in the crack were being crushed to produce that portion of the data. Digitized waveforms recorded during current test periods are being analyzed to determine if pattern recognition can distinguish between what appears to be oxide cracking and crack growth AE.

The data rates recorded just before the nozzle failure (600 to 800 events/cycle) are high enough to make source location questionable. During parts of the load cycle, there is little, if any, time separation between signals, making it difficult to obtain accurate measurements of delta-t of signal arrival at four sensors.

Data from Step 9 and the beginning of Step 11 indicate that AE was detected from the upper and lower longitudinal welds on the KSO7 replacement insert. AE was also identified from the nozzle that failed in Step 11, but it was thought to originate in the A533B insert weld. The weld was inspected and no cracking was found, but the inspection did not include the nozzle.

A concentrated effort is being applied to complete the analysis of the 70°C portion of the ZB-1 test (first half). The results will be informally presented prior to reporting on the complete test.

REACTOR MONITORING

AE monitoring of hot functional testing at the Watts Bar 1 reactor was completed. Although the data analysis is not yet complete, results appear to be very positive. The most important feature to date is the suppression of background noise from coolant flow with increasing temperature and pressure.

A representative AE sensor installation on the No. 2 inlet nozzle is shown in Figure 3. Sensors tuned to 500-kHz and 375-kHz peak response and two commercial untuned high-temperature sensors were used. The response of these sensors to coolant flow noise is shown in Figure 4. It is important to understand that the AE signal level range shown was measured from fatigue crack growth with tuned AE sensors on the ZB-1 test vessel. The material in the ZB-1 vessel is 5-in. thick A533B steel; the sensors were similar to those used at Watts Bar; and the test simulated reactor operating conditions. On this basis, it is considered legitimate to use those levels as a reference.

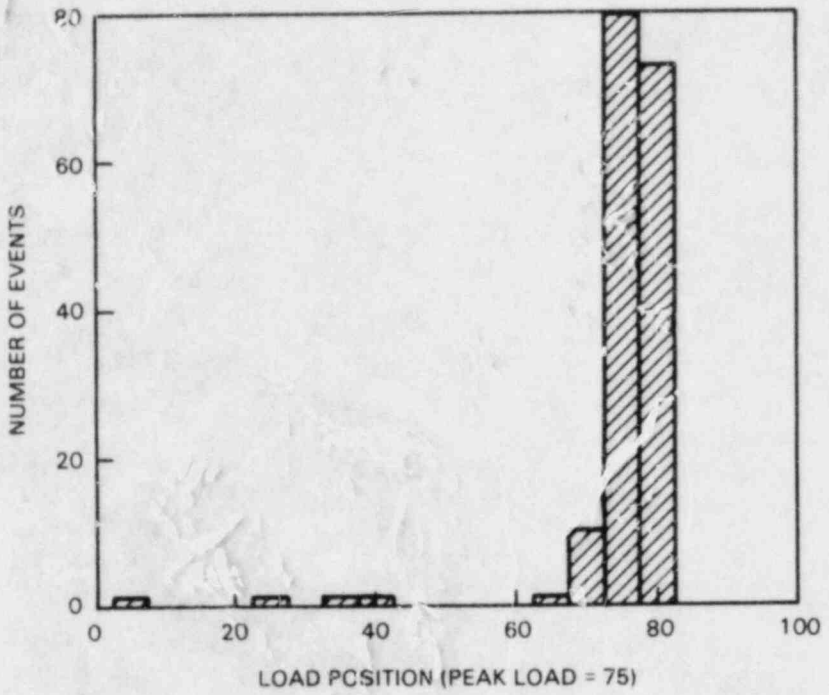

FIGURE 1. Load Position Distribution of AE Data from Flaw B in Step 5, ZB-1 Vessel Test

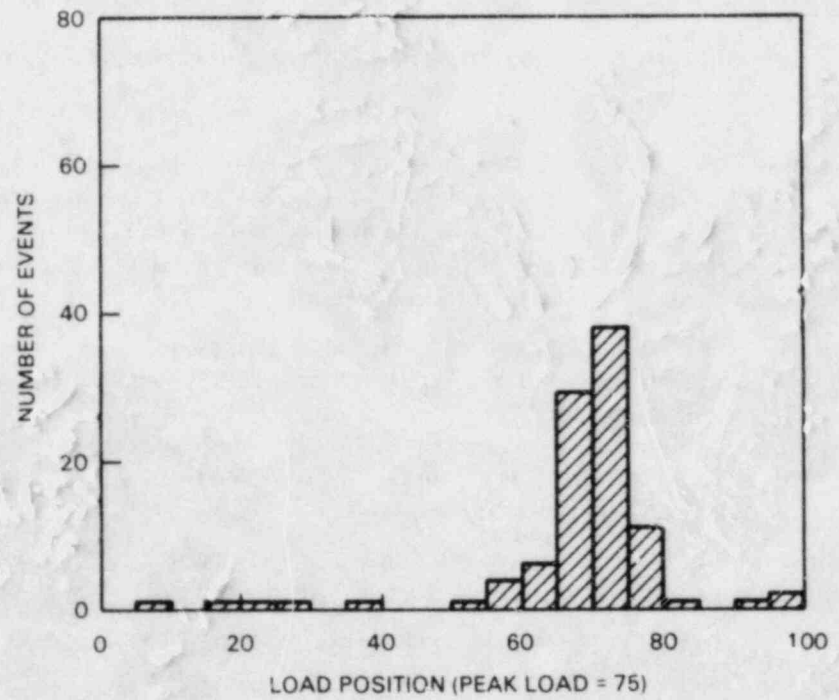

FIGURE 2. Load Position Distribution of AE Data from Flaw B in Step 6, ZB-1 Vessel Test

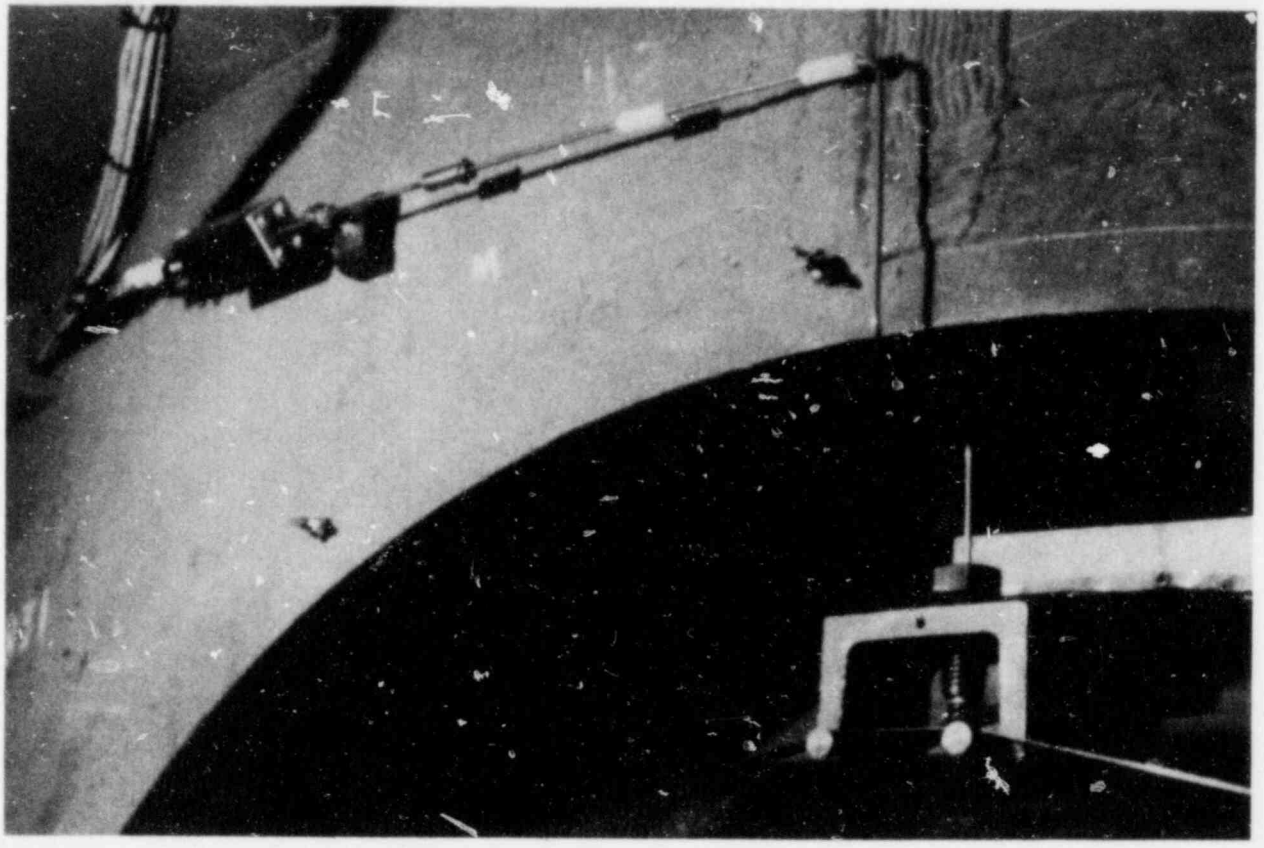

FIGURE 3. Tuned Waveguide AE Sensor Installed on No. 2 Inlet Nozzle—Watts Bar 1 Reactor

The noise at 150°F and 400 psig made AE detection highly improbable even with 500-kHz tuned sensors (Figure 4). As the coolant temperature and pressure increased, however, conditions improved dramatically. The temperature increase appears to produce a major portion of the change as illustrated by the increase to 350°F and 400 psig. At this point, the 500-kHz tuned sensors detected AE with an average signal-to-noise ratio of about 3.

As the temperature and pressure increased to 450°F and 1200 psig and above, the coolant flow noise detected by the 500-kHz sensor dropped to less than 1 volt, which should improve its AE detection effectiveness. Although the 375-kHz tuned sensor still showed an appreciable noise level (4-1/2 to 5 volts), it could be used for AE detection. The untuned high-temperature sensor appears to be very marginal for AE detection in its present form. The effectiveness of this sensor could be improved by tuning to curtail low-frequency response.

Hot functional testing results are being compiled into a report that will be reviewed by the Tennessee Valley Authority and published as a formal NRC document.

PIPE MONITORING SYSTEM

The fabrication of a compact AE system for monitoring piping weld areas is 90% complete. The objective of this task is to assemble a complete system—including sensors, sensor-mounting hardware, and cabling—that can be quickly and easily applied to a given location in a reactor.

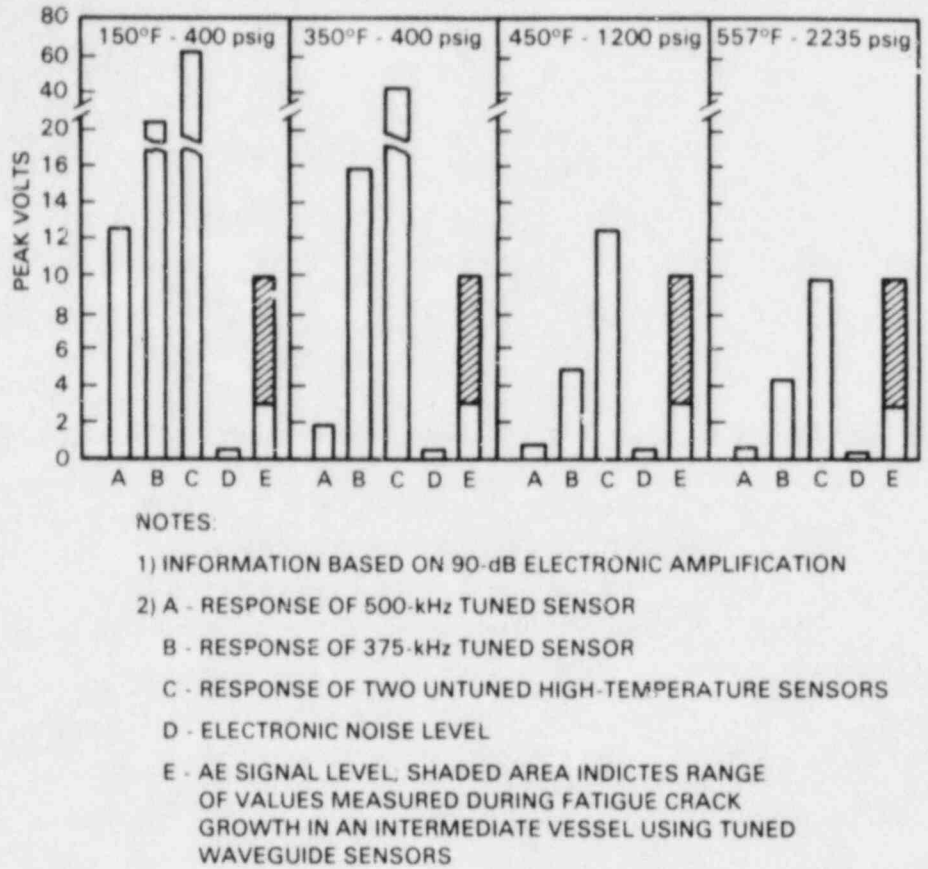

FIGURE 4. Coolant Flow Noise Versus Temperature and Pressure as a Function of Sensor Type—Watts Bar 1 Reactor

REPORTS

- Quarterly progress report for the period from April 1 to June 30, 1983.

FUTURE WORK

- Retrieve the A533B implant plus other selected specimens from the ZB-1 test vessel for metallographic examination.
- Complete a summary report on the 70°C portion of the ZB-1 vessel test.
- Complete a topical report on the AE results from hot functional testing at the Watts Bar 1 reactor.
- Continue pipe material testing.
- Summarize program activities at the 11th Water Reactor Safety Research Information Meeting.

INTEGRATION OF NONDESTRUCTIVE EXAMINATION RELIABILITY AND FRACTURE MECHANICS(a)

S. R. Doctor, Program Manager
F. A. Simonen, Project Manager
T. T. Taylor, Project Manager

L. A. Charlot
H. R. Hartzog
P. G. Heasler
G. A. Mart

SUMMARY

During the past quarter, there was one major problem that achieved high visibility: the reliable and accurate depth sizing of intergranular stress corrosion cracks (IGSCC). The efforts in the Vessel Application Task were placed on hold, and all available manpower was shifted to the Piping Application Task. The results described in this quarterly report are for the vessel and fracture mechanics (FM) tasks

INTRODUCTION

The primary pressure boundaries (pressure vessels and piping) of nuclear power plants are inspected in-service according to the rules of the ASME Boiler and Pressure Vessel Code, Section XI (Rules for In-Service Inspection of Nuclear Power Plant Components). Ultrasonic techniques are normally used for these inspections, which are periodically performed on a sampling of welds. The Integration of Nondestructive Examination (NDE) Reliability and Fracture Mechanics Program at Pacific Northwest Laboratory (PNL) was established to determine the reliability of current-in service inspection (ISI) techniques and to develop recommendations that will insure a suitably high inspection reliability. The objectives of this U.S. Nuclear Regulatory Commission (NRC) program are to:

- determine the reliability of ultrasonic ISI performed on commercial light-water reactor (LWR) primary systems
- using probabilistic FM analysis, determine the impact of NDE unreliability on system safety and determine the level of inspection reliability required to insure a suitably low failure probability
- evaluate the degree of reliability improvement that could be achieved using improved and advanced NDE techniques
- based on material properties, service conditions, and NDE uncertainties, formulate recommended revisions to ASME Code, Section XI, and Regulatory Requirements needed to insure suitably low failure probabilities.

The scope of this program is limited to ISI of primary systems, and the results and recommendations are also applicable to Class II piping systems.

(a) FIN: B2289-0; NRC Contact: J. Muscara.

TECHNICAL PROGRESS

The progress and accomplishments of the past quarter are described below by task.

VESSEL APPLICATION TASK

A preliminary evaluation of the effect of cladding type on the inspectability of near-surface underclad flaws related to pressurized thermal shock (PTS) was completed using Matrix II blocks. Matrix II test blocks have the following design:

- The six test blocks consist of three cladding types (two each): shielded metal arc weld (SMAW), three-wire submerged arc, and 2-in. strip cladding.
- All six Matrix II test blocks are 12 in. long, 12 in. wide, and ~3 in. thick. All six blocks have an ~0.25-in. thick mainly stainless steel (SS) overlay that was left "as welded" on all six blocks. Each block contains four thermal fatigue cracks (0.25 in. deep by 1.0 in. long) beneath the cladding and two 1/16-in. side-drilled holes (SDHs) at the clad/base metal interface. One SDH is parallel to the lay of the cladding and one is perpendicular. One of the strip-clad test blocks has no SDHs.

A three-pronged evaluation was conducted:

- Automated ultrasonic results were used to evaluate the effectiveness of time-amplitude locus curve principles in detecting flaws located beneath various types of cladding.
- Manual ultrasonic results were used to quantify the detectability and sizing differences for flaws located beneath various types of cladding.
- Automated profilometry provided preliminary correlations between surface roughness and inspectability of underclad flaws.

Automated Ultrasonic Results

Evidence has been presented that cladding distorts longitudinal waves less than it distorts shear waves.[1] Thus, longitudinal wave inspection techniques constitute the best mode of sound propagation for penetrating cladding and detecting underclad flaws. Furthermore, geometric considerations dictate the use of high inspection angles for optimal defect detection. Therefore, this quarter's research concentrated on comparing the detectabilities of cracks under various types of cladding, using high-angle longitudinal inspections exclusively.

Detectability using time-amplitude locus curve criteria requires that the time-of-flight of the flaw echo must vary directly and linearly with the distance of the transducers from the flaw. Furthermore, the amplitude of the flaw echo must remain higher than the background noise over sufficiently long amounts of probe motion to be visually distinguishable from spurious indications (see Figures 1, 2, and 3). The stringency of this latter criterion might conceivably be relaxed if the flaws were to be searched for computationally rather than visually (as in SAFT processing).

Using the time-amplitude locus technique, a 5-MHz focused immersion transducer detected thermal fatigue cracks under both the three-wire and strip claddings, using insonification directions either parallel or perpendicular to the lay of the cladding. However, this equipment failed to detect thermal fatigue cracks under the SMAW cladding. Using the same technique with a 2-MHz zone-isolated contact transducer on the SMAW cladding detected cracks when insonified parallel to the lay of the cladding but failed to detect cracks that required insonification perpendicular to the lay.

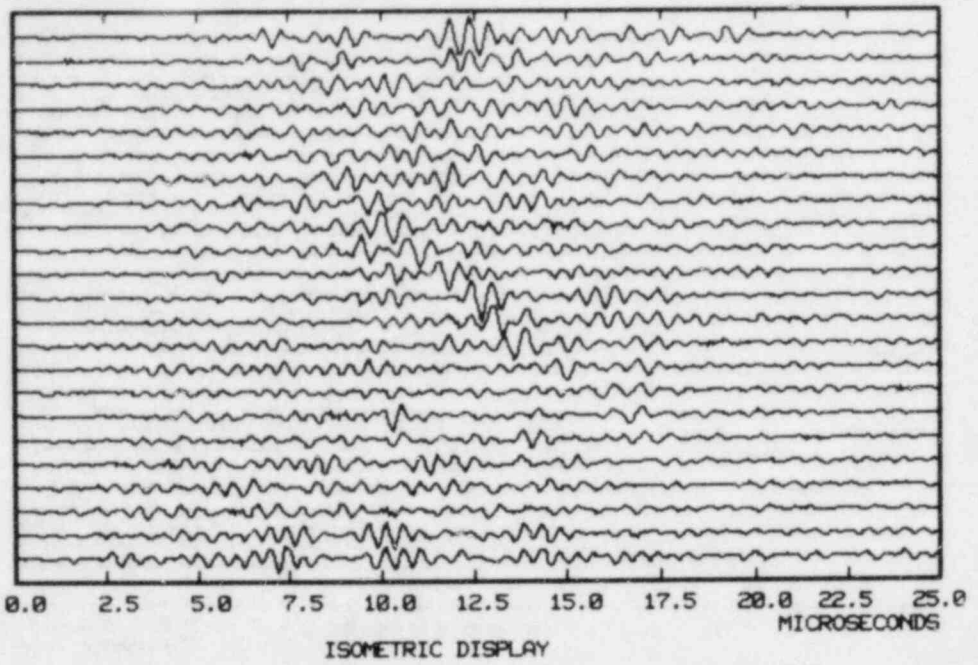

FIGURE 1. Nominal 0.25-in. Deep Thermal Fatigue Crack Under Shielded Metal Arc Weld Cladding Scanned Parallel to the Lay of the Cladding

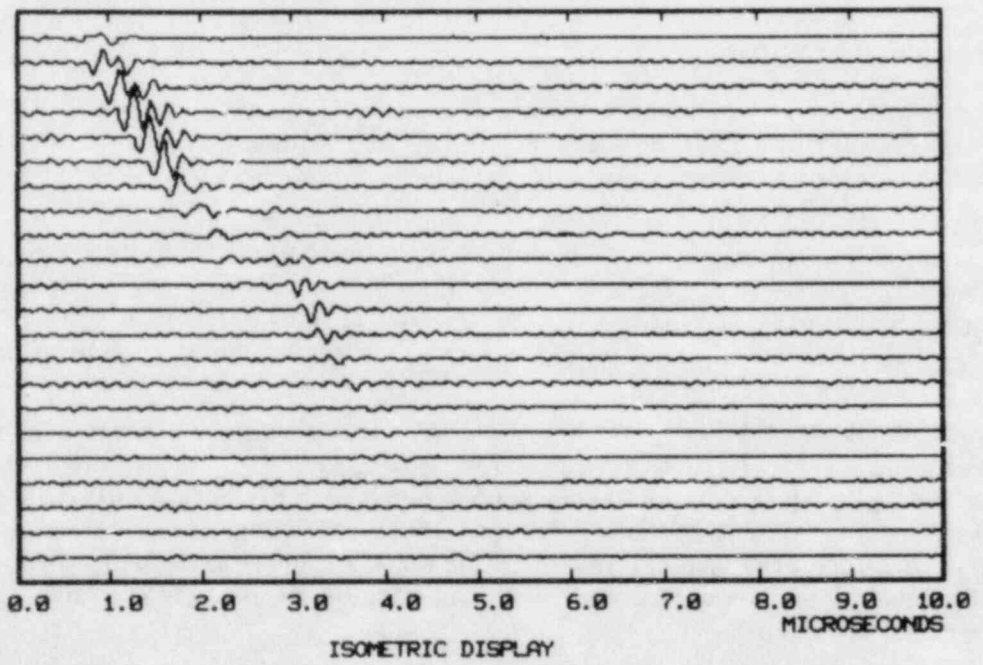

FIGURE 2. Nominal 0.25-in. Deep Thermal Fatigue Crack Under Three-Wire Submerged Arc Cladding Scanned Perpendicular to the Lay of the Cladding

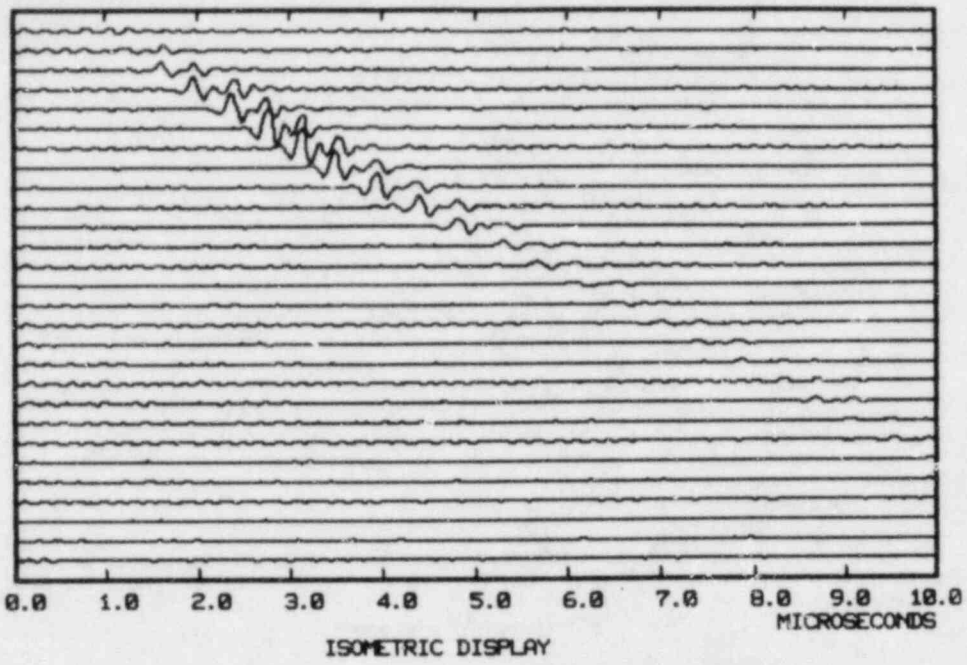

FIGURE 3. Nominal 0.25-in. Deep Thermal Fatigue Crack Under 2-in. Strip Cladding Scanned Perpendicular to the Lay of the Cladding

Manual Ultrasonic Results

Three zone-focusing transducers with beam angles of 70°, 60°, and 45° were used for the manual ultrasonic evaluation. The 2-MHz, dual-element, pitch-catch transducers had a contact surface ~1.0 in. by 1.0 in. Maximum focusing occurred ~0.23 in. in the steel for the 70° unit, 0.6 in. deep for the 60° unit, and 0.7 in. deep for the 45° unit.

The manual ultrasonic evaluation was calibrated using a carbon steel Navships block to generate a distance-amplitude curve (DAC). The reference level for each cladding type was set by adjusting the instrument gain to yield 100% DAC from the reflected signal of a 1/16-in. SDH. Signal amplitudes from other defects were then reported relative to the reference level (+ above; - below) in decibels.

Table 1 shows the detectability of the Matrix II thermal fatigue cracks as a function of cladding type. Each crack was inspected separately from each side. At best, 55% of the cracks were detected in the block with SMAW cladding; 100% of the cracks were detected in blocks with three-wire submerged arc and strip cladding. Amplitude-based detection of SMAW cladding overlay in the as-welded condition is, therefore, not reliable; three-wire submerged arc and strip claddings yield a surface condition suitable for reliable detection of underclad cracks in the as-welded condition for amplitude-based detection.

The ability to size underclad cracks as a function of cladding type is shown in Table 2. Underclad cracks can be accurately sized through three-wire submerged arc and strip cladding but not through as-welded SMAW cladding.

TABLE 1. Thermal Fatigue Cracks Detected in Matrix II Test Blocks Using 70°, 60°, and 45° Transducers

	Shielded Metal Arc Weld Cladding			3-Wire Submerged Arc Cladding			Strip Cladding		
	70°	60°	45°	70°	60°	45°	70°	60°	45°
No. of cracks detected	8	9	5	16	16	16	16	16	16
No. of cracks not detected	8	7	11	0	0	0	0	0	0
Average amplitude of detected cracks,(a) dB	-5.1	-5.4	-4.8	+2.2	-4.1	-9.6	+1.4	-4.1	-6.9

(a) Relative to distance-amplitude curve.

TABLE 2. Sizability of Underclad Cracks in Matrix II Test Blocks Using 60° and 45° Transducers

	Shielded Metal Arc Weld Cladding		3-Wire Submerged Arc Cladding		Strip Cladding	
	60°	45°	60°	45°	60°	45°
No. of cracks sizable(a)	0	0	13	16	15	16
No. of cracks not sizable	16	16	3	0	1	0

(a) Sizable is defined as being able to clearly recognize the bottom tip signal, which is used to size underclad cracks. Sizing error is expected to be less than 20% but cannot be determined without destructive testing.

Tables 3 and 4 indicate the deviation in signal amplitude associated with several 1/16-in. SDHs as a function of cladding type. All SDHs were located at the clad/base metal interface, and the recorded amplitude is the maximum amplitude attained without effects from the edge of the test block. The tables show the consistency/repeatability trends that could be expected using a given calibration reflector intended to standardize examination sensitivity. As expected, the strip cladding (predominantly smooth) yields a small deviation and, thus, a repeatable calibration sensitivity and a standardized examination for underclad cracks. The SMAW cladding yields as much as a 15-dB spread (5.0-dB average for 60° transducer) in signal amplitude, reducing the standardization of examination sensitivity. The three-wire submerged arc cladding also yielded a small deviation in signal amplitude from the 1/16-in. SDHs.

TABLE 3. Average Deviation of Signal Amplitude from 1/16-in. SDH Reference Reflectors

Transducer	Shielded Metal Arc Weld Cladding	3-Wire Submerged Arc Cladding	Strip Cladding
70° SEL	3.7 dB	1.7 dB	1.0 dB
60° SEL	5.0 dB	2.3 dB	1.0 dB
45° SEL	3.9 dB	2.0 dB	2.4 dB

TABLE 4. Amplitudes of All 1/16-in. SDHs Relative to Reference Reflector

Transducer	Shielded Metal Arc Weld Cladding	3-Wire Submerged Arc Cladding	Strip Cladding
70° SEL	-6, -7, 0, -1, -8, -2, -2	+3, +3, 0, +2, +2, +1, -1	+1, +1, +1
60° SEL	-9, -4, 0, +2, -13, -3, -4	-2, -5, +2, -2, -4, 0, +1	-2, 0, -1
45° SEL	+6, +4, +1, +6, 0, +4, +6	-2, -4, 0, -4, -6, -1, 0	0, +2, +4

Automated Profilometry Results

The surfaces of each of the three types of cladding were profiled using a linear variable differential transformer. Profiles were taken perpendicular to the lay of the cladding to provide conservative estimates of the roughness of each cladding type. The results are given in Table 5.

TABLE 5. Surface Roughness Results

Cladding	RMS Surface Roughness,(a) mils
Automatic 2-in. strip	2.6
Automatic three-wire submerged arc	8.9
Single-strand shielded metal arc	11.5

(a) Root mean square.

FRACTURE MECHANICS ANALYSES

FM analyses apply deterministic and probabilistic FM to the development of ISI requirements. Critical factors of concern include: NDE sensitivity requirements, inspection intervals, and weld inspection sampling plans. Analyses have been performed to evaluate the impact of NDE on system safety and reliability. The studies described below address SCC, thermal fatigue, and weld inspection sampling plans.

Impact of NDE on IGSCC

Probability of crack detection curves (Figure 4) from the PNL piping inspection round robin were applied to data on IGSCC from the EPRI/BWR Owners' Group Research Project[2,3] as indicated in Figures 5 and 6. The results (Figure 7) indicate that a significant increase in reactor piping reliability can result from improved NDE and that improved NDE can result in enhanced detection of IGSCC without offsetting requirements for shorter ISI intervals.

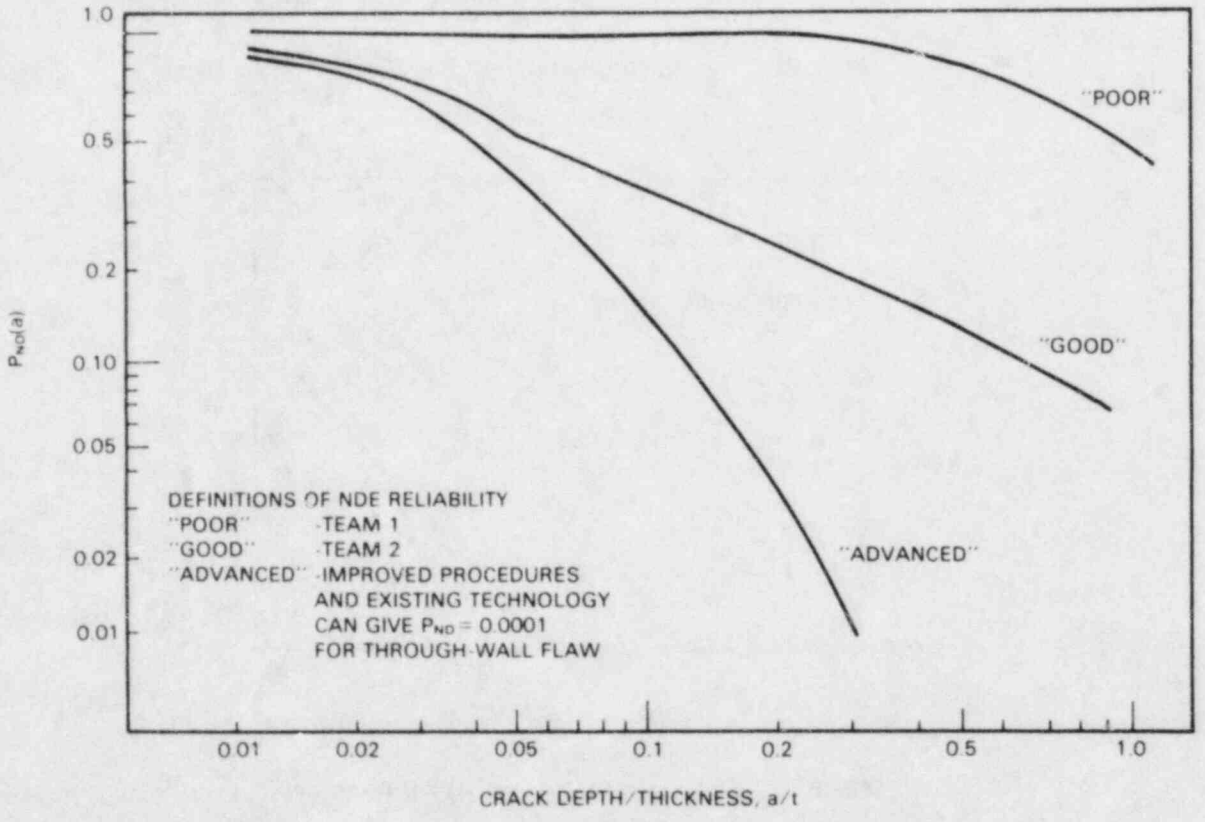

FIGURE 4. Detection of IGSCC in 10-in. Stainless Steel Pipe

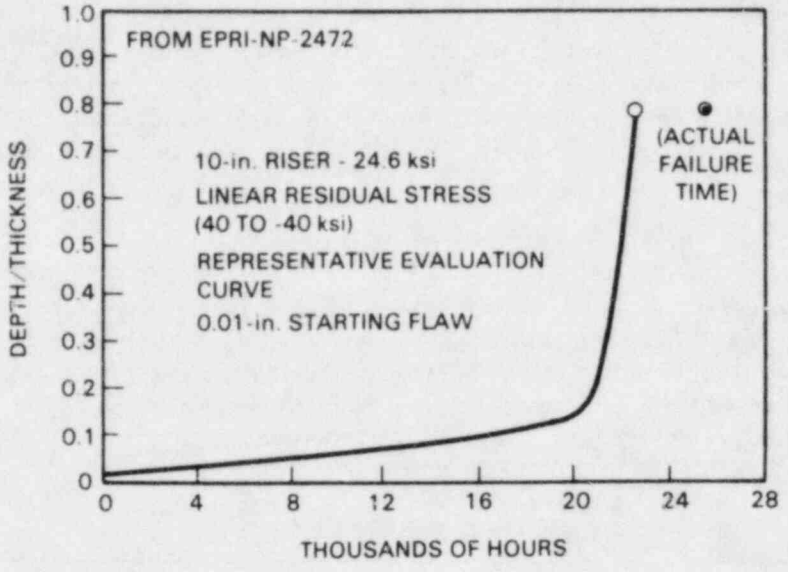

FIGURE 5. Predicted Growth of IGSCC

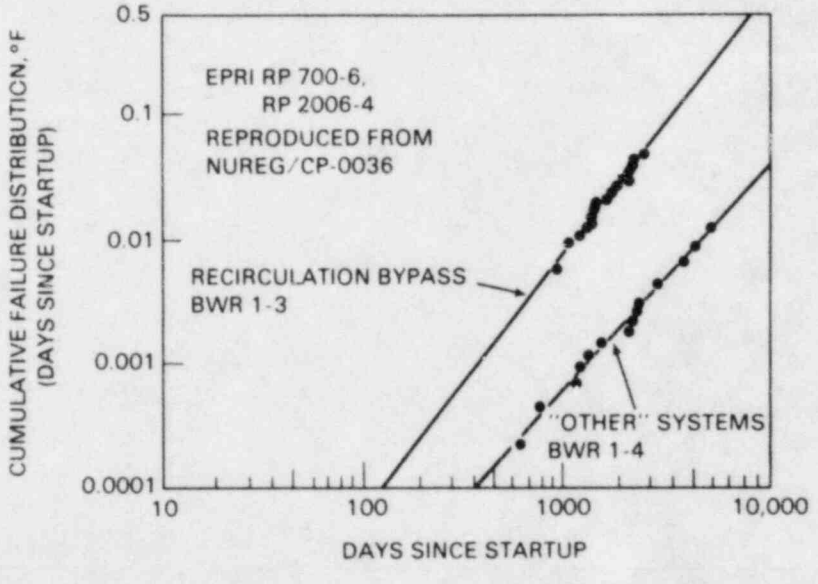

FIGURE 6. IGSCC Experience in BWR Piping

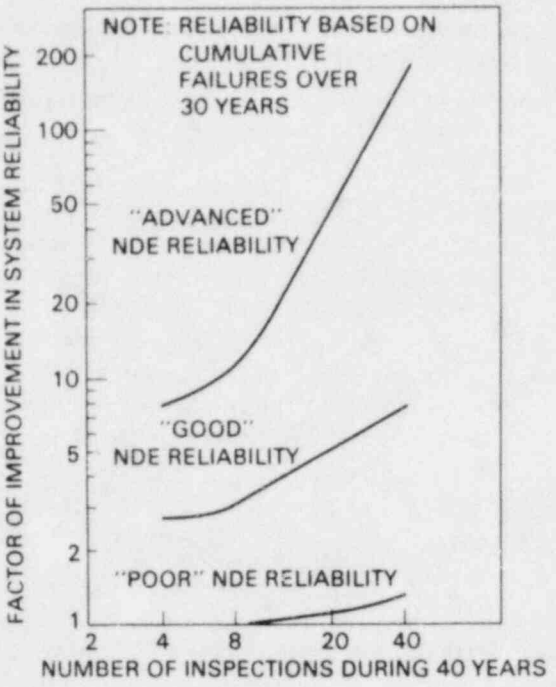

FIGURE 7. Predicted Impact of NDE on the Occurrence of Leaks Due to IGSCC

The calculations used the crack growth curve of Figure 5, which was extracted from Reference 3. While this curve is based on extensive analytical developments and experimental laboratory programs, it must be recognized that any prediction of the progress of IGSCC is subject to considerable uncertainty and is the topic of continuing research efforts. The key feature of the particular curve in Figure 5 is the prolonged period of shallow crack depth (from an initial depth of 0.010 in.) and the slow crack growth rate over most of the life of the component. Under these conditions, detecting relatively shallow cracks is difficult. If the probability of detection is to be high, the inspection must occur after the crack depth has increased to a more detectable size. The crack depth versus time curve of Figure 5 was not used in an absolute sense. Only the shape of the curve was applied in probabilistic calculations.

The actual time for a through-wall crack was assumed to be described by the statistical distribution shown in Figure 6. This distribution[4] was empirically derived from an analysis of data from field experience with BWR piping systems. The curves in Figure 6 show the fraction of welds that have required repair due to IGSCC; this fraction increases with time as the days of reactor operation increase. Data fell into two populations, designated as recirculation bypass lines and "other" BWR systems.[4] There is considerable weld-to-weld variation in service life, which can be attributed to differences in welding residual stresses, coolant system chemistry, degree of sensitization from welding, and other unspecified factors.

The probability of flaw nondetection curves in Figure 4 for "poor" and "good" NDE reliability represent the range of performance by different teams in the PNL piping inspection round robin. The "advanced" curve is an estimate of the level of performance that can be achieved within the limitations of field procedures and existing technology. For IGSCC, there is clearly a significant range in team-to-team performance, although all teams met minimum ASME Section XI Code requirements. The "poor" team detected only ~10% of flaws as deep as 40% of the wall thickness.

In contrast, the "good" team detected ~80% of the flaws 40% deep. The "advanced" curve assigns a 10^{-4} probability of nondetection for a through-wall flaw, assuming that advanced instrumentation will be used and that human errors will be the major factor in nondetection of deep flaws. For small flaws, the instrumentation and physics of the detection process will be the major factors. A 90% probability of detection for a 10% deep flaw was assumed.

In the FM calculations it was necessary to apply the detection curves outside the parameters of the piping inspection round robin. For pipe wall thicknesses other than the 10-in. Schedule 80 pipe of the round robin, it was assumed that the detection probability was a function of the a/t ratio, with the same curve applying to all wall thicknesses. The round robin did not involve repeated inspection of actual growing IGSCC flaws. For multiple inspections, a lower bound on detection probability was estimated using methods from reliability theory. The detection probability was taken as the best obtained in any of the multiple inspections or, in effect, that for the last inspection where the crack was the deepest. An alternative approach is to assume an optimistic upper bound behavior governed by the product of the probabilities of nondetection from the successive inspections. This approach is believed to be overly optimistic because it does not properly account for the systematic factors that may impede the detection of a given crack (e.g., crack tightness).

For the calculations of Figure 7, the 40-year life was divided into uniform inspection intervals; and inspections were performed at the midpoint of each interval. ISI intervals ranging from 10 years (ASME Code-scheduled inspection) to 1 year were considered. In the probabilistic calculations, a distribution of crack growth curves of the shape shown in Figure 5 was simulated, with the end points of the curves having the distribution shown in Figure 6.

The impact of NDE on system reliability is shown in Figure 7. Reliability is based on the number of leaks that occur over the 40-year design life of the plant. The factor of improvement is defined as:

$$\text{Factor of Improvement} = \frac{\text{Number of Leaks Without NDE}}{\text{Number of Leaks With NDE}}$$

The predicted improvement in system reliability increases as the number of inspections over the 40-year design life increases. It appears that "poor" NDE has little impact on system reliability but that "good" NDE can improve reliability by a factor of 2 to 10 depending on the ISI period. Even greater potential benefits can be achieved with "advanced" technology and procedures. In particular, the frequency of inspection required by NUREG-0313 and the elimination of ineffective ISI via IEB 83-02 provide a factor of improvement of ~5 over code-minimum ISI as provided by the "poor" NDE reliability curve (Figure 4). The calculations of the impact of NDE on IGSCC support the following conclusions:

- There are clear and significant differences in the ability of both present and improved NDE procedures to detect IGSCC before leaking occurs.
- The "poor" team cannot approach a 50% probability of detecting IGSCC prior to leaking, even with an extremely short inspection interval (once per year). Inspections of this quality are essentially of zero benefit and are not justified on the bases of cost and radiation exposure.
- The "good" team can readily achieve a factor of 2 improvement in preventing leaks due to IGSCC and can, with a short inspection interval, approach a factor of 10 improvement.
- "Advanced" ISI can readily achieve a factor of 10 improvement in preventing IGSCC leaks; this factor can be increased to 100 by sufficiently decreasing the ISI interval.

- Better inspection procedures ("good" versus "poor" and "advanced" versus "good") appear to offer a cost-effective option for enhancing piping performance. The results indicate that using better procedures can be more effective than a ten-fold increase in the number of inspections using an inferior procedure.
- A factor of 10 decrease in failure probability can be viewed as a reasonable goal for the benefit that can be achieved through ISI.
- The results show that relatively short inspection intervals (one inspection per year of operation) are required to prevent leaks due to IGSCC in failure-prone welds. Such inspection intervals may be a practical but temporary measure for a few selected welds. Such intervals would be impractical as a plant-wide measure to assure piping integrity.

Piping Reliability Using the PRAISE Code

PNL piping inspection round robin data have been used in probabilistic FM calculations being performed for PNL by Lawrence Livermore National Laboratory (LLNL) using the computer code PRAISE.[4] Previously developed crack growth models at LLNL have been revised to permit the simulation of alternate inspection scenarios.

The revised models include the simulation of initial flaws that are representative of long but shallow service-induced cracks rather than fabrication flaws in welds. Fatigue crack and IGSCC growth rate curves have been developed to represent the variability seen in experimental growth rates. Alternate inspection scenarios have been evaluated using probability of detection curves based on the PNL piping inspection round robin.

Inspection of ferritic piping has been addressed using a model that simulates cracking that has occurred by thermal fatigue in PWR steam generator feedwater lines.[5] The impact of NDE on IGSCC is being addressed using a model of the cracking of the Duane Arnold safe ends.[5] In each case, the inspection scenario considers a range of inspection intervals and probability of detection curves.

In the model of the PWR feedwater lines, the following set of inspection scenarios has been evaluated:

- two plants: high and typical failure probabilities
- ASME ISI Programs A and B
- four inspection intervals: ASME, 10 years, 5 years, and 1 year
- three detection probabilities: poor, good, and advanced.

The flaw detection curves shown in Figure 8 are based on the PNL round robin data for clad ferritic piping. The data were extrapolated to treat:

- flaws less than 5% of the wall thickness
- pipe wall thicknesses less than 2.375 in.
- enhanced detection through improved procedures and technology.

Typical results of the LLNL calculations for PWR feedwater lines using the PRAISE code are shown in Figure 9. As indicated, the predicted leak probability is high, which correlates with service experience. After 10 years of operation, the predicted failure probability approaches 90%. For this situation, inspections late in life (at 10 years) are of little benefit. As the ISI period is decreased, the benefit of NDE (decrease in leak probability) increases substantially. The relative benefits of

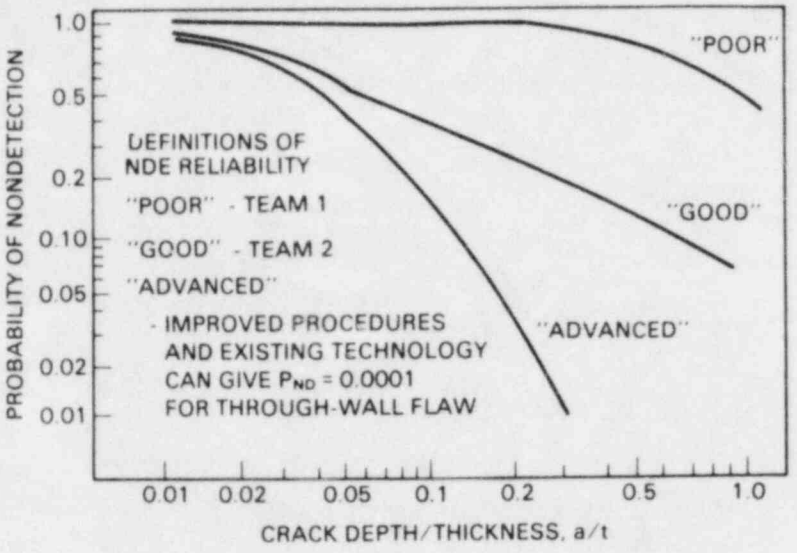

FIGURE 8. Probability of Flaw Nondetection for Ferritic Piping

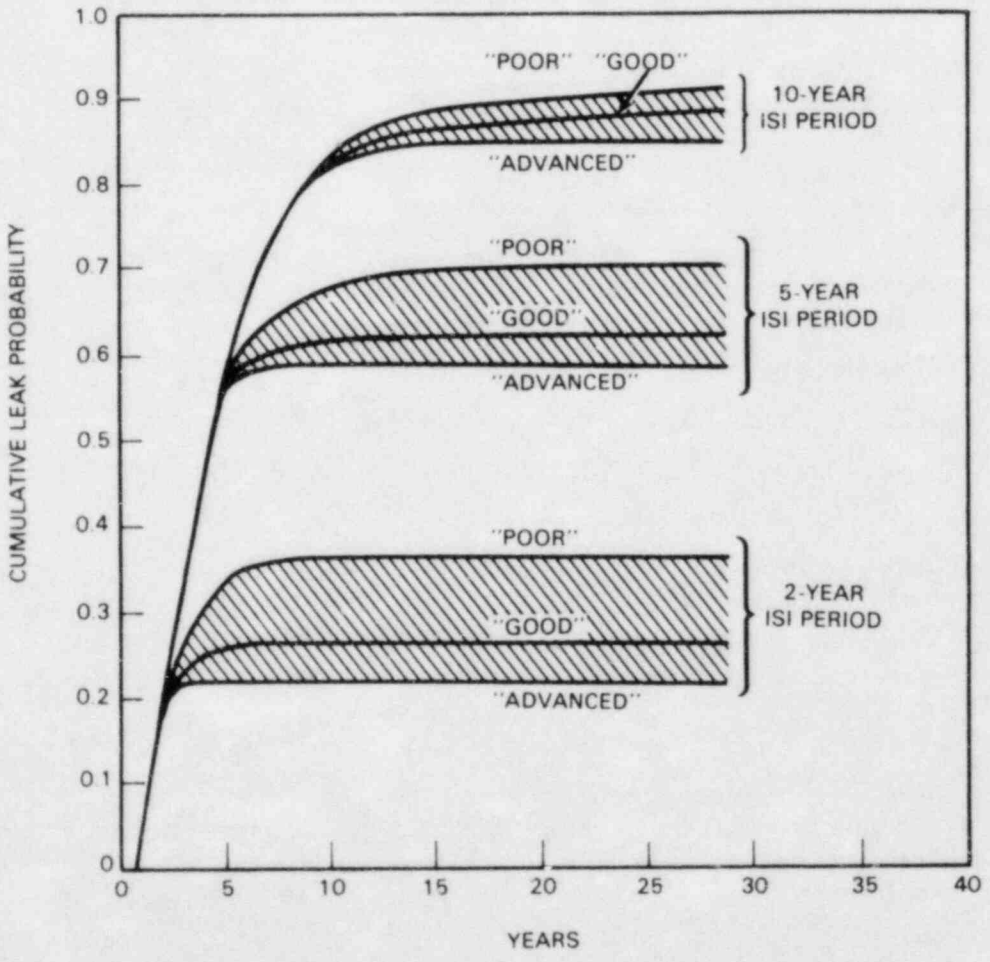

FIGURE 9. Thermal Fatigue of PWR Feedwater Nozzle—LLNL Piping Reliability Calculations Using PRAISE Code

enhanced NDE reliability ("poor" versus "good" versus "advanced") are not as evident as the calculations for IGSCC (Figure 7) due to the following factors:

- The variation of performance in NDE reliability ("poor" to "advanced") is not nearly as great for ferritic piping (Figure 8) as for IGSCC in SS piping (Figure 4). For ferritic piping, even the "poor" inspections were relatively effective.
- The PWR feedwater line scenario involved very high failure probabilities early in the design life. In such situations, the effectiveness of ISI is evidently dominated by the ISI period rather than the probability of detection curve that characterizes the NDE reliability. The NDE reliability does, however, have a significant impact on the slope of the curves after the first inspection (Figure 9); the failure rate decreases substantially.
- Certain assumptions of the probabilistic model in the PRAISE code tend to minimize the apparent differences between the "poor" to "advanced" NDE reliability. Defective piping that either leaks or has detectable cracks is assumed to be replaced with "perfect" material that is immune to future crack growth. In addition, crack nondetection is assumed to be entirely the result of random factors, rather than systematic causes as was assumed for the IGSCC calculations.

Weld Inspection Sampling Plans

Calculations have been performed using a PNL model of weld inspection sampling plans for piping systems to estimate a factor of improvement in system reliability that can be attributed to ISI. The effectiveness of the ASME Code sampling plan has been compared with alternative plans that require fewer or greater numbers of inspections.

For present ISI requirements for piping, only a sample of the welds in a system must be inspected. If flaws are detected, then additional welds must be inspected. The overall effectiveness of the inspection depends on selecting a sufficient number of critical welds in the inspection sample.

Probabilistic methods have been applied to estimate the degree of NDE unreliability that results when less than 100% inspection is performed. To focus on the impact of sample plans, these calculations assume that all flaws will be detected in a timely manner in any weld that is inspected in accordance with the inspection plan.

Table 6 shows factors of improvement for various inspection scenarios where:

$$\text{Factor of Improvement} = \frac{\text{Failure Rate Without Inspection}}{\text{Failure Rate with Inspection}}$$

TABLE 6. Estimated Factors of Improvement in Reliability for Alternate Weld Inspection Sampling Plans

Surveillance Inspection Plan	Scenario 1	Scenario 2	Scenario 3
ASME Code	2.16	4.32	4.32
None	1.00	1.60	1.77

In these calculations, the failure rates (leak rates) were those calculated in Reference 4 for 14 critical welds in a PWR primary coolant loop. The plan for scheduled inspections was consistent with ASME Section XI requirements. Three scenarios, each corresponding to a different action to be taken when a failure occurs in an uninspected weld, were considered:

- Scenario 1 - no additional inspection
- Scenario 2 - 100% inspection of the failed weld in the other three loops of the plant
- Scenario 3 - 100% inspection of the failed weld in all loops in each of 20 similar plants that constitute the population of concern.

It was also assumed that 50% of the failures were random in character and that the remainder were systematic failures evenly divided between those problems specific to one plant and those problems generic to all 20 plants of the population.

As indicated in Table 6, the ASME Code sampling plan gave a predicted improvement factor of ~4.0 at best. This factor assumed that fully augmented inspection was performed and that the NDE procedures detected all flaws in inspected welds. In contrast with no scheduled inspection plan (augmented inspection only), the maximum factor of improvement is less than 2.0.

The variation in predicted improvement factors as a function of changes in the relative fractions of random versus systematic failures (both of the design/population wide and plant specific types) is shown in Table 7. The impact of augmented inspection is dramatic (a factor of improvement of 43.21) when the failures are largely systematic rather than random in nature. Furthermore, the factors of improvement show a progressive increase as the level of both scheduled and augmented inspections increases.

TABLE 7. Estimated Factors of Improvement as a Function of Changing Fractions of Design, Plant, and Random Failures

Code-Scheduled Inspection for All 20 Plants

Fraction of Failure Types					
Design	Plant	Random	Scenario 1	Scenario 2	Scenario 3
0.05	0.05	0.90	2.16	2.40	2.40
0.05	0.90	0.05	2.16	43.21	43.21
0.90	0.05	0.05	2.16	43.21	42.31

No Scheduled Inspection for All 20 Plants

Fraction of Failure Types					
Design	Plant	Random	Scenario 1	Scenario 2	Scenario 3
0.05	0.05	0.90	1.00	1.081	1.095
0.05	0.90	0.05	1.00	3.478	3.628
0.90	0.05	0.05	1.00	3.478	13.560

FUTURE WORK

- Complete the pipe inspection round robin report.
- Place cracks in other pipe specimens.
- Evaluate techniques for providing more accurate crack depth sizing information.
- Complete the special study report on centrifugally cast stainless steel in which Westinghouse participated.

REFERENCES

1. Edler, S. K., ed. 1983. *Reactor Safety Research Programs Quarterly Report, April-June 1983.* NUREG/CR-3307, Vol. 2, PNL-4705-2, Pacific Northwest Laboratory, Richland, Washington.

2. General Electric. July 1982. *The Growth and Stability of Stress Corrosion Cracks in Large-Diameter BWR Piping.* NP-2472, prepared by General Electric Company for BWR Owner's Group and Electric Power Research Institute.

3. Eason, E. D. 1982. "Stress Corrosion Cracking in Boiling Water Reactor (BWR) Piping." In *Proceedings of the Workshop on Nuclear Power Plant Aging,* August 4-5, 1982, Bethesda, Maryland, NUREG/CP-0036.

4. Harris, D. O., E. Y. Lim, and D. D. Dedhia. August 1981. *Probability of Pipe Fracture in the Primary Coolant Loop of a PWR Plant, Volume 5: Probabilistic Fracture Mechanics Analysis.* NUREG/CR-2189, U.S. Nuclear Regulatory Commission, Washington, D.C.

5. Woo, H. H. 1982. "Piping Reliability Model Development, Validation and Its Application to Light Water Reactor Piping." Presented at the Tenth Water Reactor Safety Research Information Meeting, October 10-15, 1982, Gaithersburg, Maryland.

EXPERIMENTAL SUPPORT AND DEVELOPMENT OF SINGLE-ROD FUEL CODES[a]

D. D. Lanning, Program Manager

D. D. Lanning, Task A Leader
M. E. Cunningham, Task B Leader
W. N. Rausch, Task C Leader
J. O. Barner, Task D Leader

E. R. Bradley
R. J. Guenther
R. E. Williford

SUMMARY

The principal objectives of this program are to obtain in-reactor and out-of-reactor data on thermal and mechanical fuel rod performance and to integrate these data into the FRAPCON-2 computer code. During this quarter, electron probe microanalysis (EPMA) and thermocouple osmium content data were received from the postirradiation examination (PIE) of IFA-432. The final corrections to the IFA-527 PIE report were completed. The fission gas release model PARAGRASS was linked with FRAPCON-2, tested, and found to perform similarly to the FRAPCON-2/FASTGRASS combination.

INTRODUCTION

The objectives of the Experimental Support and Development of Single-Rod Fuel Codes Program at Pacific Northwest Laboratory (PNL) are fourfold:

- Task A - collect and correlate in-reactor and PIE data on fuel rod thermal/mechanical behavior, especially as a function of rod design and burnup
- Task B - qualify, organize, and analyze the fuel performance data and report the data, trends, and conclusions
- Task C - integrate the above information into the FRAPCON series of computer codes
- Task D - study the occurrence and mechanisms of cladding deformation and failure using controlled experiments with centrally heated simulated fuel rods in a pressurized water loop at PNL.

The Halden Boiling Water Reactor (HBWR), Halden, Norway, is currently the sole site used by this program for irradiation tests. PIE is being conducted at the AERE-Harwell[b] laboratories in the United Kingdom. The in-reactor test matrix now spans the full range of normal BWR conditions for pelletized UO_2 fuel, including:

- powers up to 50 kW/m (16 kW/ft)
- diametral gap sizes of 50 to 380 μm (0.002 to 0.015 in.)
- initial gas compositions ranging from pure helium to pure xenon

---

(a) FIN: B2043; NRC Contact: H. H. Scott.
(b) Atomic Energy Research Establishment.

- fuel densities of 95% and 92% of theoretical density (TD), the latter both stable and unstable regarding in-reactor densification
- burnups to 52 MWd/kgM
- alternate fuel designs (annular fuel pellets, coated cladding, and sphere-pac fuel).

Five instrumented test assemblies have been irradiated thus far in the program. Two of the assemblies—IFA-432 and IFA-518—are still under irradiation.

TECHNICAL PROGRESS

Work that has been completed during this quarter is discussed by task in the following sections.

TASK A - IRRADIATION EXPERIMENTS

The irradiation of IFA-432 and IFA-518 continued during the quarter. The burnup increment for the period from July 16, 1983, to September 30, 1983, was approximately 1.0 MWd/kgM for IFA-432 and 1.5 MWd/kgM for IFA-518. Fuel rod instrumentation continued to operate satisfactorily.

Additional PIE data from Rods 1 and 6 of IFA-432 were received from Harwell and included ceramography, EPMA, and scanning electron microscope (SEM) results. Results of the chemical analysis of W/Re thermocouple wires for end-of-life composition were also received. These results are discussed under Task B

TASK B - DATA QUALIFICATION AND ANALYSIS

Analysis of Fission Gas Release Data for IFA-432

Rods 1, 5, and 6 of IFA-432 were instrumented with pressure transducers to monitor the internal pressure changes that occurred during irradiation. The pressure data (obtained up to 30 MWd/kgM rod-average burnup) have been used to estimate fission gas release as a function of burnup. Rod puncture data and retained gas measurements are also available from the PIE of Rods 1 and 6. These experimental data are being compared with calculations based on fission gas release models that are currently used in the FRAPCON-2[1] computer code.

Fission gas release calculations have been made using certain versions of the FASTGRASS and PARAGRASS gas release models that were developed at Argonne National Laboratory. In making the calculations, the temperature and power histories were the same as those used in comparing other fission gas release models with the IFA-432 data.[2,3] The results of the present gas release calculations at 10, 20, and 30 MWd/kgM are compared with the experimental estimates derived from pressure and PIE data in Table 1.

Calculations based on FASTGRASS show reasonable agreement with the experimental estimates for all three fuel rods. The calculated end-of-life gas release is slightly below the PIE measurement for Rod 6 and somewhat higher than measured for Rod 1. The calculations also show reasonable agreement with the burnup dependence derived from the in-reactor pressure data. PARAGRASS calculations also show good agreement with the experimental estimates for Rod 6 but severely underestimate gas release from Rod 1. The difference between the two gas release model calculations appears to be related to the much stronger grain size dependence in PARAGRASS. The average grain diameter near the pellet center of fuel in Rod 1 was 60 μm compared with 10 μm for fuel in Rod 6 and 15 μm for fuel in Rod 5. Comparing the calculated gas releases from the two models at 30 MWd/kgM shows the difference in gas release increases with the fuel grain size, which indicates a stronger dependence on grain size in PARAGRASS.

Both models show good agreement with the measured radial distribution for the total retained fission gas in pellet 41 of Rod 6 (see Figure 1). The experimental values were obtained by dissolving

TABLE 1. Comparison of Experimental Fission Gas Release Estimates from IFA-432 with Calculated Releases from FASTGRASS and PARAGRASS

Rod	Burnup, MWd/kgM	Experimental Gas Release Estimates, (a) %	Gas Release from PIE, %	Calculated Gas Release, % FASTGRASS	Calculated Gas Release, % PARAGRASS
1	10	2 to 4		2.1	0.1
	20	5 to 8		6.6	0.6
	30	4 to 6(b)	5 to 6	9.7	1.0
5	10	8 to 12		5.9	5.4
	20	6 to 10		8.1	6.1
	30	6 to 10		10.0	6.1
6	10	9 to 14		7.4	11.6
	20	9 to 14		13.0	15.4
	30	9 to 15(c)	19 to 20	16.9	16.5

(a) From in-reactor pressure data.
(b) End-of-life best estimate = 4.1%.
(c) End-of-life best estimate = 14.7%.

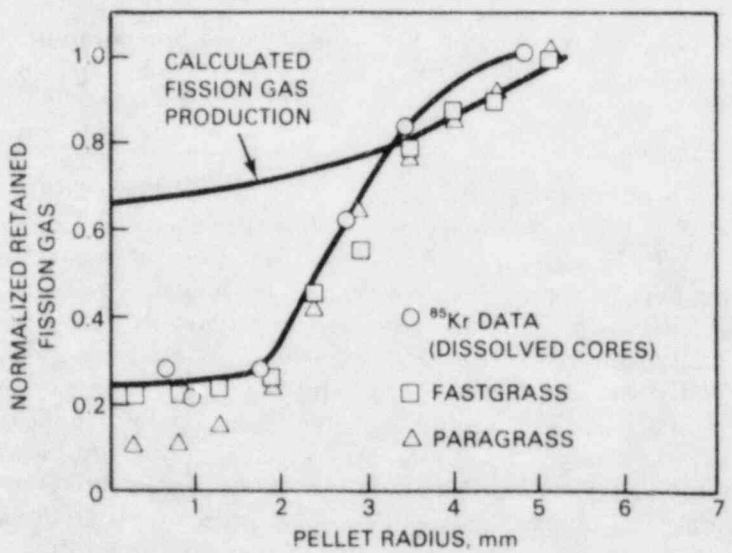

FIGURE 1. Radial Distribution of Total Retained Fission Gas—Comparison of Experimental and Calculated Values.

small fuel cores taken at selected radial positions and measuring the amount of ^{85}Kr released to obtain a relative measure of the total retained gas. The ^{85}Kr data and the calculated concentrations were normalized to the peak concentrations that occurred near the pellet edge. Both models predict that measurable fission gas release will begin at about 1100°C and will increase with increasing fuel temperature (see Figure 2). There are small differences in the calculated radial gas distributions between the two models. Better agreement between the model predictions and the data would be obtained if the normalization were done at a radius of about 4.8 mm.

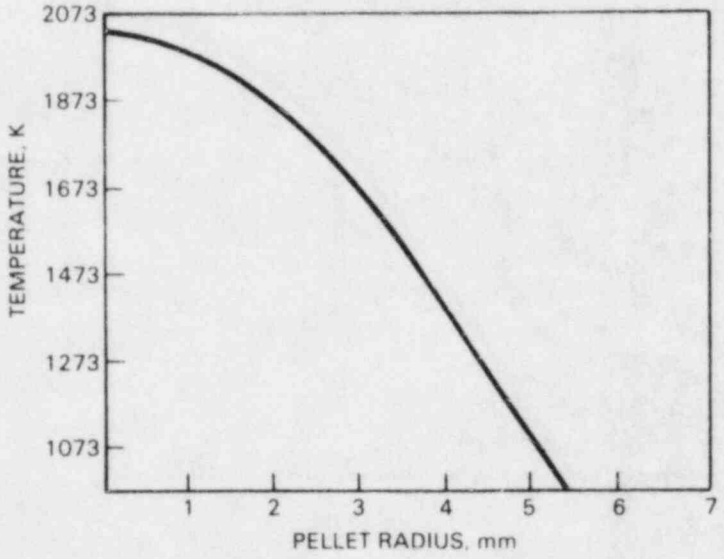

FIGURE 2. Fuel Radial Temperature Profile for Comparison with Retained Fission Gas Radial Distributions

Although both models predict similar total fission gas releases and radial distributions for the total retained gas in pellet 41 of Rod 6, differences exist in the predicted partition of retained fission gas between that within the fuel grains (intragranular) and that stored at grain boundaries (intergranular). A comparison has been made between the calculated radial distributions for intragranular and intergranular retained fission gas and that deduced from experimental measurements on pellet 41 of Rod 6. EPMA scans across the pellet diameter were used to determine the radial distribution of the intragranular retained gas. The EPMA data and the calculated intragranular concentrations, normalized to the respective pellet edge concentrations, are compared in Figure 3. The intergranular retained fission gas was experimentally estimated by microcoring, crushing half-cores, and measuring the activity of the ^{85}Kr released. These data and the calculated intergranular fission gas concentrations, normalized to the pellet edge values, are presented in Figure 4.

FASTGRASS fission gas release model predictions agree more closely with the experimental distributions for both intergranular and intragranular retained gas than the PARAGRASS predictions. The intergranular retained fission gas data from the crushed cores and the FASTGRASS calculations show a peak in intergranular gas storage at about midradius. The difference in the peak magnitudes (Figure 4) is somewhat misleading because it significantly depends on the uncertainty of the intergranular gas concentration near the pellet edge. However, Figure 4 does highlight the difference between the data and the calculations.

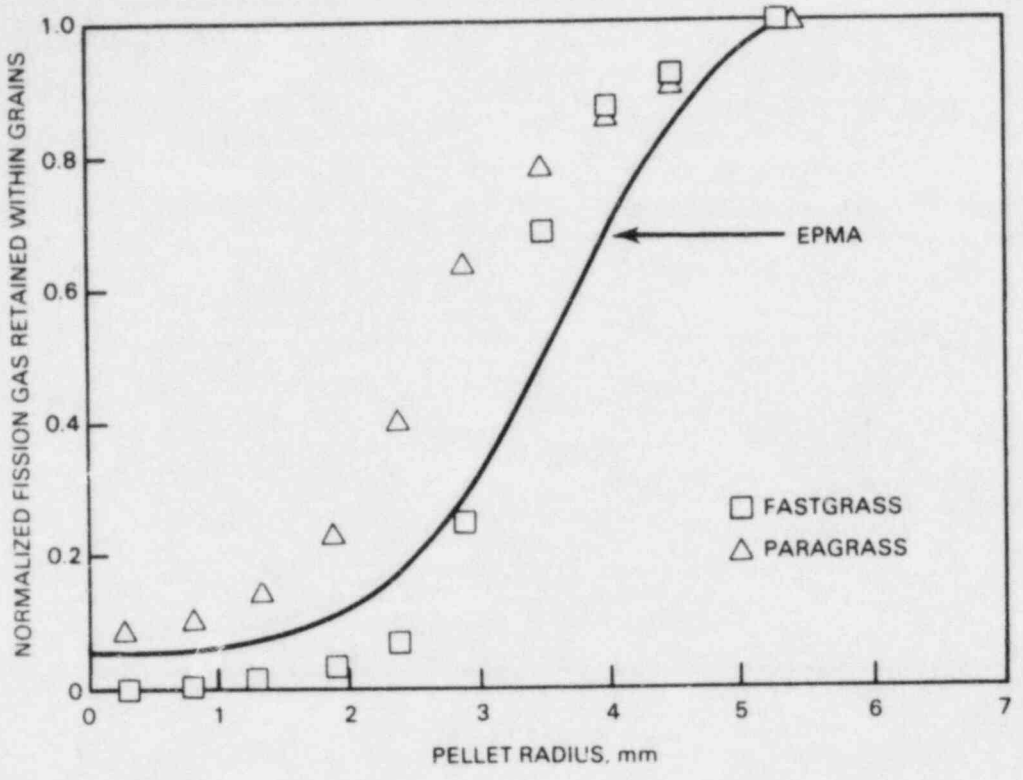

FIGURE 3. Radial Distribution of Intragranular Fission Gas—Comparison of Experimental and Calculated Values

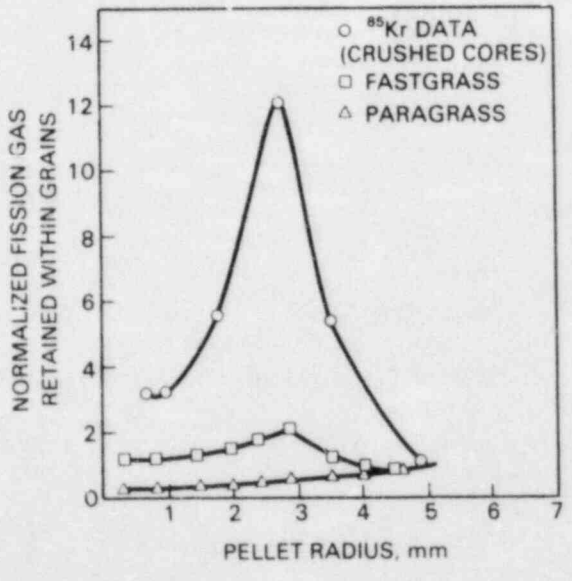

FIGURE 4. Radial Distribution of Intergranular Fission Gas—Comparison of Experimental and Calculated Values

The remaining half-cores from the same radial locations were dissolved and the ^{85}Kr activity was measured, which enabled the total relative retained gas to be determined (Figure 1). The relative intergranular fission gas fraction was assumed to be the ratio between the ^{85}Kr activity released by crushing and by dissolution. Compared with the data, FASTGRASS predicted that a greater fraction of the total retained gas near the pellet edge is stored at grain boundaries (Figure 5). Both FASTGRASS calculations and the experimental ^{85}Kr data indicate that about 80% of the retained gas near the midradius position is located at grain boundaries.

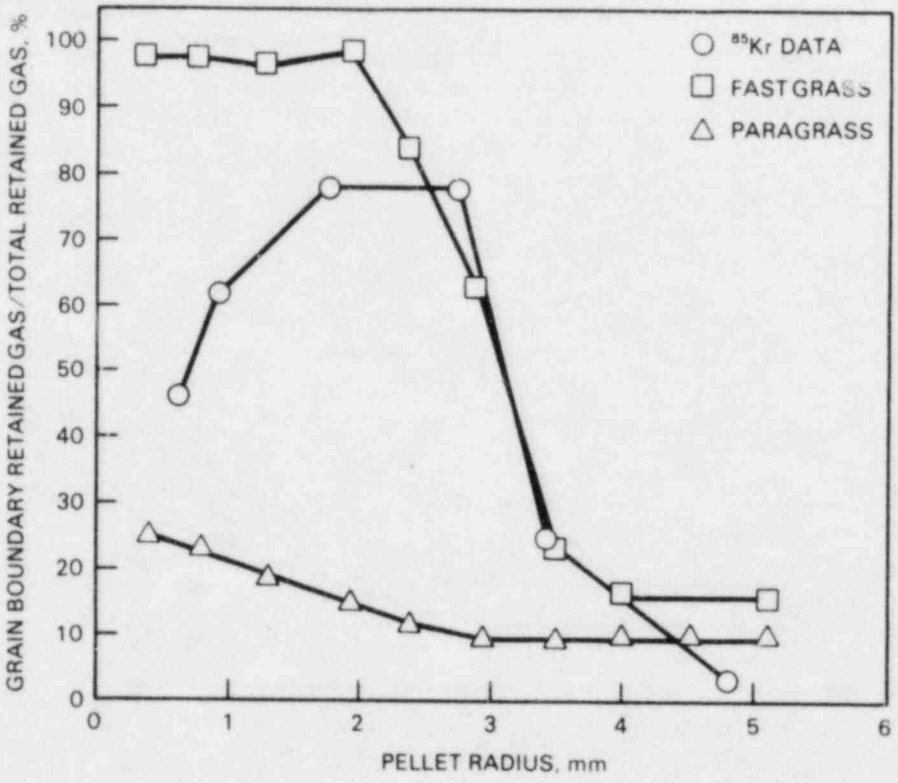

FIGURE 5. Fractional Grain Boundary Storage for Pellet 41 of Rod 6

In contrast with the FASTGRASS calculations, the PARAGRASS calculations indicated that the intergranular gas concentration increases continuously with increasing radius (Figures 4 and 5). The calculated fraction of the retained gas stored at grain boundaries was also well below the experimental measurements for all but the outermost regions of the fuel pellet.[a] Because PARAGRASS generally underpredicts the intergranular fraction, it therefore overestimates the intragranular fraction relative to both FASTGRASS and the data (Figure 3).

(a) Compared with the data, PARAGRASS (like FASTGRASS) overpredicted the intergranular retained fission gas for the outer fuel regions (Figure 5).

Chemical Analysis of Irradiated Thermocouples

The lower fuel thermocouple from Rod 1 of IFA-432 was analyzed for osmium content (Table 2). Osmium, which is formed by transmutation from rhenium, affects thermocouple voltage output and results in a decalibration with increasing neutron fluence. A shielding effect by the fuel on the thermocouple probably accounts for the 20% difference between samples from inside the fuel and a sample from outside the fuel.

The measured osmium content has been compared with a calculation for osmium generation.(4) The calculation assumed a 26% Re/74% W wire in a constant thermal neutron flux to a fluence of 3×10^{22}. This calculation compares well with the measured content considering the uncertainties in interpolating the calculated curves down to the small actual fluence (8×10^{20} n/m^2).

TABLE 2. Measured Osmium Content of Lower Thermocouple from Rod 1 of IFA-432

Distance from Thermocouple Tip, cm	Osmium in W-5% Re Leg, at .%	Osmium in W-26% Re Leg, at .%
1.6(a)	0.24 ± 0.02	0.97 ± 0.05
3.9(a)	0.25 ± 0.02	1.00 ± 0.05
6.3(a)	0.23 ± 0.02	0.98 ± 0.05
8.7(b)	0.26 ± 0.02	1.20 ± 0.05

(a) Inside fuel.
(b) Just outside fuel.

IFA-527 Analysis

Final modifications to the IFA-527 PIE report were completed. PIE results for visual examination, neutron radiography, leak testing, water content analysis, and optical metallography are included in the report. A primary conclusion from the PIE results is that operating in the failed condition (at less than 20 kW/m peak power) had little effect on the fuel and cladding of rods from IFA-527.

The cladding leak test indicated that all rods leaked in the region of the end fittings and not in the cladding. The water content analysis for Rod 4 found a significant amount of D_2O, indicating that water ingress occurred during irradiation and not in the cooling pond following irradiation.

Neither neutron radiography nor optical metallography of Rods 1 and 4 provided any evidence of cladding hydriding. The observable hydriding was comparable with that found for Rod 8 of IFA-432, which obtained a burnup of 20 MWd/kgM without failure.

IFA-518 Analysis

Low-power cladding elongation and gas pressure data for IFA-518 rods were collected in July 1983 and compared with data collected before May 1983. All instrumentation appears to be operating correctly; and the July data basically match extrapolations of previous data trends, except for the cladding elongation for two rods. Rod ACP-32 had elongated 100 μm above the expected value, and

Rod A-7 had increased 25 μm. It should be noted that the peak pellet linear heat generation rate for the assembly has increased to approximately 40 kW/m for the upper cluster rods and 32 kW/m for the lower cluster rods.

TASK C - FUEL CODE MAINTENANCE AND IMPROVEMENT

The PARAGRASS fission gas release model was linked to FRAPCON-2 and tested on a variety of input cases. In general, the code performed similarly to the FRAPCON-2/FASTGRASS combination, although it was discovered that PARAGRASS is much more sensitive to fuel grain size than FASTGRASS. The two models also differ in the fraction of retained gas that they predict to occur within grains.

The Idaho National Engineering Laboratory supplied PNL with a copy of the revised FRACAS-II fuel rod mechanical model as it now exists in FRAP-T6 (Version 13). This new version of FRACAS-II will replace the one currently included in FRAPCON-2. It appears that this change will require a major effort because the FORTRAN structures have been changed considerably.

TASK D - PELLET-CLADDING INTERACTION EXPERIMENTS

A summary of the paper "Ex-Reactor PCI Experiments" was prepared for the Eleventh Water Reactor Safety Research Information Meeting. This summary provided information related to the five electrically heated fuel rod experiments that used irradiated Zircaloy cladding.

FUTURE WORK

Planned activities for the next quarter include further analysis of the IFA-432 data, continued work on the IFA-432 PIE report, and completion of the IFA-527 PIE report.

REFERENCES

1. Berna, G. A., et al. 1981. *FRAPCON-2: A Computer Code for the Calculation of Steady-State Thermal-Mechanical Behavior of Oxide Fuel Rods.* NUREG/CR-1845, Idaho National Engineering Laboratory, Idaho Falls, Idaho.
2. Edler, S. K., ed. March 1982. *Reactor Safety Research Programs Quarterly Report, October-December 1981.* NUREG/CR-2127, Vol. 4, PNL-3810-4, Pacific Northwest Laboratory, Richland, Washington.
3. Edler, S. K., ed. September 1982. *Reactor Safety Research Programs Quarterly Report, April-June 1982.* NUREG/CR-2716, Vol. 2, PNL-4275-2, Pacific Northwest Laboratory, Richland, Washington.
4. Herzfeld. 1962. *Temperature.* Vol. 3, Part 2. Reinhold Publishing, New York.

ACCELERATED PELLET-CLADDING INTERACTION MODELING[a]

R. E. Williford, Project Manager

M. E. Cunningham
D. D. Lanning

SUMMARY

The first working version of the fuel failure code was completed on July 29, 1983. Sample cases were presented to U.S. Nuclear Regulatory Commission (NRC) staff in early August.

INTRODUCTION

This Pacific Northwest Laboratory (PNL) program is divided into two tasks with the following objectives:

- Task A - to complete a pellet-cladding interaction (PCI)-related fuel failure model for NRC policy use, to assess the model, and to report the results.
- Task B - to obtain or develop an improved burnup-dependent model for predicting pellet radial power profiles to be used in the NRC fuel behavior code FRAPCON-2.

Fuel failure modeling draws upon previous work performed under FIN B2043, where cracked fuel mechanical behavior models were developed. With the addition of cladding damage and statistically oriented models, the resulting code will predict the probability of fuel rod failure under normal reactor operating conditions and for events described by Chapter 15 of the Safety Analysis Review.

For Task B, PNL has obtained the computer code RADAR[b] for use in FRAPCON-2 or related codes. RADAR calculates the changing pellet radial power profile as a function of ^{235}U burnup and ^{239}Pu production.

TECHNICAL PROGRESS

The progress that was made in each task during this quarter is described below.

TASK A - FUEL FAILURE MODELING

Four major components have been developed and implemented in the fuel failure code (GT2-F): a transient temperature calculator; a mechanical model to describe the cladding stress concentrations caused by cracked fuel pellets; a submodel for corrodent (iodine, ZrI_4) release and/or inventory during steady-state and transient conditions; and three cladding fracture process submodels.

The transient temperature submodel was completed and implemented. A new constitutive equation was developed for the mechanical model to properly account for the effects of the nonlinear mechanical behavior of cracked fuel on cladding ridge formation. Results of this submodel show that the largest cladding stress concentrations are not always associated with the smallest gap size

---

(a) FIN: B2452; NRC Contact: H. H. Scott.
(b) Developed by British Nuclear Fuels Limited.

for a given fuel rod power rating. The steady-state corrodent (iodine) gas release model was developed from the ANS 5.4 fission gas release model and accounts for the decay of unstable isotopes. The transient iodine release model is based on the direct electrical heating experiments performed at Argonne National Laboratory.

Two cladding fracture process submodels were developed and implemented; these submodels describe 1) nonchemically assisted (slower) creep cracking and 2) chemically assisted (faster) stress corrosion cracking (SCC). These two submodels represent the lower and upper bounds of possible cladding fracture mechanisms.

The third fracture submodel produces a best-estimate calculation and describes the transition between the other two fracture submodels as the corrodent concentration increases. This submodel treats iodine depletion by chemical reaction to form ZrI_4, diffusion of ZrI_4 down the crack, adsorption at the crack tip and subsequent embrittlement of the Zircaloy, crack tip damage, crack initiation time, crack growth rates, crack arrest, and a displacement-controlled crack growth option. This model reproduces the strain rate sensitivity and failure time characteristics of Zircaloy/iodine laboratory SCC data. Results show that the Zircaloy/iodine SCC process is dominated by chemical reaction and creep rates, rather than by a threshold stress or diffusion times. SCC begins at very low iodine concentrations, and crack tip chemical processes may be fast enough to be similar to liquid metal embrittlement phenomena. Failure times are dominated by the time required to initiate active crack growth.

At NRC's request, the first working version of the fuel failure code was completed in late July 1983. The results of a ramp test simulation at 30 GWd/MTM are shown in Table 1. The results indicate that the fracture submodels can adequately bound ramp test data and can adequately simulate failure events given the proper initial flaw size.

TABLE 1. Ramp Test Simulation

Initial Flaw Depth, μm	Time Required to Initiate Crack Growth, s		Time to Failure, [a] s		Crack Depth/Wall Thickness [b]	
	Best-Estimate Model	Upper Bound Model	Best-Estimate Model	Upper Bound Model	Best-Estimate Model	Upper Bound Model
25	55	—	75 (NF)[c]	40	0.042	0.107
37	10	—	10 to 15	25	0.135 to 0.253	0.117
50	1/2 SS[d]	—	ENDSS[e]	15	0.630	0.106

(a) From beginning of ramp.
(b) Immediately prior to unstable crack growth.
(c) NF = no failure.
(d) 1/2 SS = halfway through steady-state period (15 GWd/MTM).
(e) ENDSS = end of steady-state period (30 GWd/MTM).

TASK B - RADIAL POWER PROFILES

The final report for this task was issued on June 6, 1983, and concluded the activities of this task. No further work is planned.

FUTURE WORK

A cladding crack nucleation model will be developed and implemented to describe the formation of the initial flaw. Work will continue on the statistical submodel and on benchmarking, verification, and documentation of the fuel failure code.

PIPE-TO-PIPE IMPACT[a]

M.C.C. Bampton, Project Manager

J. M. Alzheimer
J. R. Friley
F. A. Simonen

SUMMARY

During the last two quarters, preliminary results were obtained from the plastic hinge study, a review of potential pipe whip arrangements was completed, and the initial test matrix was completed.

INTRODUCTION

The objective of the Pipe-to-Pipe Impact Program is to provide the U.S. Nuclear Regulatory Commission (NRC) with experimental data and analytical models for making licensing decisions regarding pipe-to-pipe impact following postulated breaks in high-energy fluid system piping. Current licensing criteria—as contained in Standard Review Plan (SRP) 3.6.2, "Determination of Break Locations and Dynamic Effects Associated with Postulated Rupture of Piping"—will be evaluated. Data will be obtained from a series of tests in which selected pipe specimens with appropriate energies will be impacted against stationary specimens to achieve required damage levels.

This Pacific Northwest Laboratory (PNL) program involves two main areas: obtaining experimental data and developing predictive models. Preliminary analyses to determine significant test parameters and required energies and pipe velocities have been completed. The test matrix has been developed; a system capable of accelerating the pipe has been built; and the test facility has been designed. The current phase of the program encompasses the actual testing. Predictive models that are analytically based and/or empirical fits of the data are being developed and will be compared with current licensing criteria.

TECHNICAL PROGRESS

Progress made during the last two quarters is discussed below by topic.

PLASTIC HINGE LOCATION STUDY

An analytic study was undertaken to investigate the location of plastic hinge formation following a postulated pipe break. Both closed form and finite element methods were used. Although the results are still preliminary, it appears that the concept of a plastic hinge forming at a single location is not valid. For the range of parameters investigated, the pipes deformed plastically over a wide region and did not deform appreciably more at any one location.

Only straight pipes were considered for the study. The effects of elbows or other attachments at the end of the pipe were ignored from a structural standpoint. However, the jet thrust was assumed to be normal to the pipe just as if it were caused by flow from an elbow. The jet thrust was assumed to be equal to the inside cross-sectional area times the initial pressure times a thrust coefficient of 1.26.

(a) FIN: B2383; NRC Contact: G. Weidenhamer.

If it is assumed that the pipe is rigid/plastic and that the shear force at the hinge is zero, a closed form solution can be derived for the position of the hinge. This distance, as measured from the end of the pipe where the thrust is applied, is three times the plastic moment divided by the thrust force. This distance is independent of the density of the pipe. For typical pipe schedules and pressures, this distance ranges from a few to several diameters, but it is less than typical support spacings.

The above closed form solution is restricted because of the assumptions required. In addition, it is probably valid only for the initial deformation phase. A finite element study was undertaken to obtain better information on the plastic deformation behavior of a whipped pipe. The ANSYS code was used; and a large displacement, elastic/plastic, transient dynamic model was developed. The wall thickness-to-diameter ratio and the internal pressure were varied. A nominal 6-in. diameter and 10-ft length were used for the initial models along with the material properties for A106 Grade B at 550°F. Selected time steps were sufficiently small to assure acceptably small plastic strain increments.

The initial results from the finite element study indicate that a plastic hinge does not form at a single location. Instead, the pipe plastically deforms over a wide region from the fixed end to near the tip. The development of the plastic region depends on the internal pressure and schedule of the pipe. However, the deformation has not been limited to a single location in any of the cases examined thus far.

PIPE WHIP SPACING STUDY

A study was undertaken to assess the distribution of piping configurations that are typical of pipe-to-pipe impact scenarios of safety-related piping in a nuclear power plant. A scale model of a nuclear power plant was used in this study. The scale model showed all safety-related piping inside containment. Pipe break locations, which had been postulated using NRC-acceptable criteria, were shown on the model. At each postulated break location, the presence of potential target pipes was noted. For the purposes of this study, pipe whip restraints were ignored and engineering judgment was used to predict whip directions. For each postulated impact event, the diameters, wall thicknesses, and material of both target and swinging pipes were recorded along with the separation distance and the relative angle of impact.

Data from this study are shown in Figures 1 and 2. Figure 1 shows the number of pipes of each diameter that were observed. Most of the swinging (impactor) pipes were 2, 3, and 12 in. in diameter with a lesser number at other diameters. Figure 2 shows the distribution of diameter and wall thickness ratios. The regions defined by the current SRP 3.6.2 criteria regarding postulated leaks and breaks and the PNL tests completed to date are also shown in Figure 2.

The data obtained in this study will be combined with other information to be used in formulating the fiscal 1984 test matrix. Key parameters will be diameter and wall thickness ratios and estimated impact energies.

INITIAL TEST MATRIX RESULTS

The initial test matrix has been completed. No data were obtained that showed the current SRP criteria to be unconservative. Two impactor pipes ruptured during testing; however, these pipes ruptured under conditions that would have required the postulation of a break by the SRP criteria. A few tests were conducted for pipe diameter and wall thickness combinations that would have required the postulation of leaks or breaks by the SRP criteria but that did not leak or break during testing.

To more efficiently plot the data, a set of normalized parameters was developed (Table 1). Data for the entire initial test matrix are shown in Figures 3 and 4. Figure 3 shows the trends in bend angles, and Figure 4 shows the trends in diameter changes.

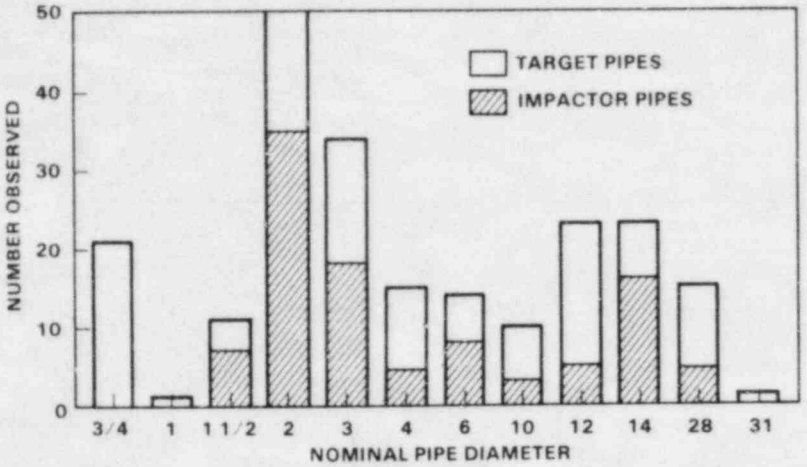

FIGURE 1. Histogram of Pipe Diameter Data

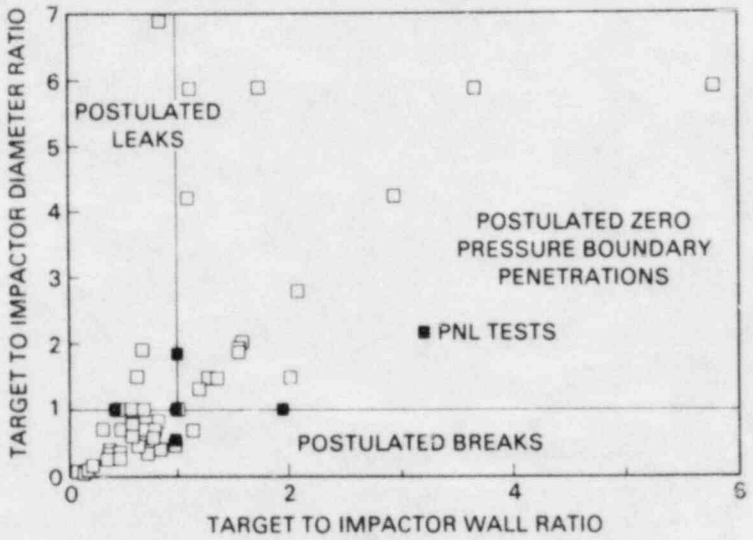

FIGURE 2. Distribution of Pipe Geometric Ratios

TABLE 1. Normalized Parameters

$$\text{Normalized impact energy} = \frac{\text{Kinetic Energy at Impact}}{\pi \sigma_z \cdot D_1 D_2 (T_1 + T_2)}$$

$$\text{Normalized diameter change} = \frac{|\Delta D_1|\Delta + |\Delta D_2|\Delta}{D_1 + D_2}$$

$$\text{Normalized bend angle} = \frac{\Theta_1 + \Theta_2}{\pi/2}$$

where σ_z = yield strength of pipe

D_1, D_2 = target and impactor pipe diameters

T_1, T_2 = target and impactor pipe wall thicknesses

$\Delta D_1, \Delta D_2$ = change in diameters

Θ_1, Θ_2 = target and impactor pipe bend angles.

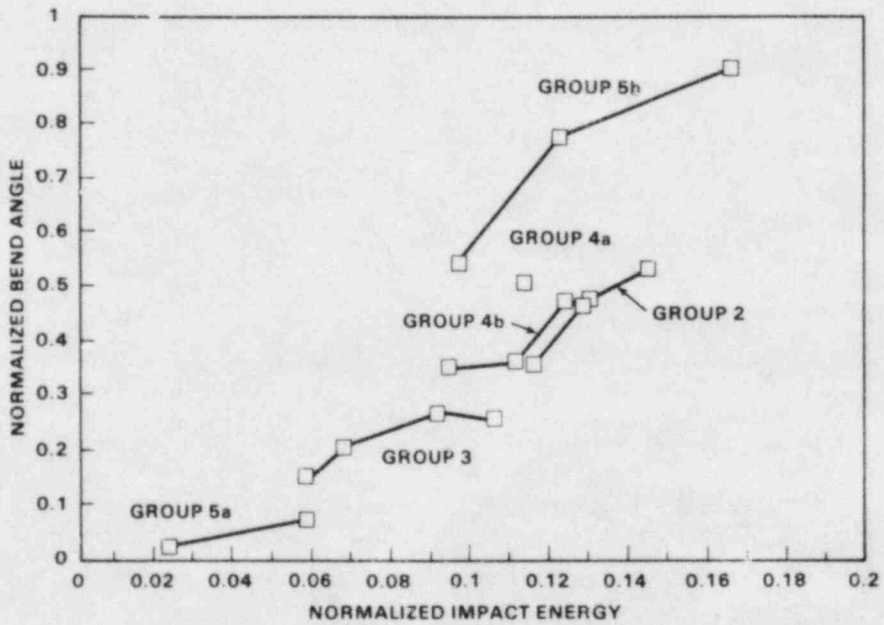

FIGURE 3. Normalized Bend Angle Data

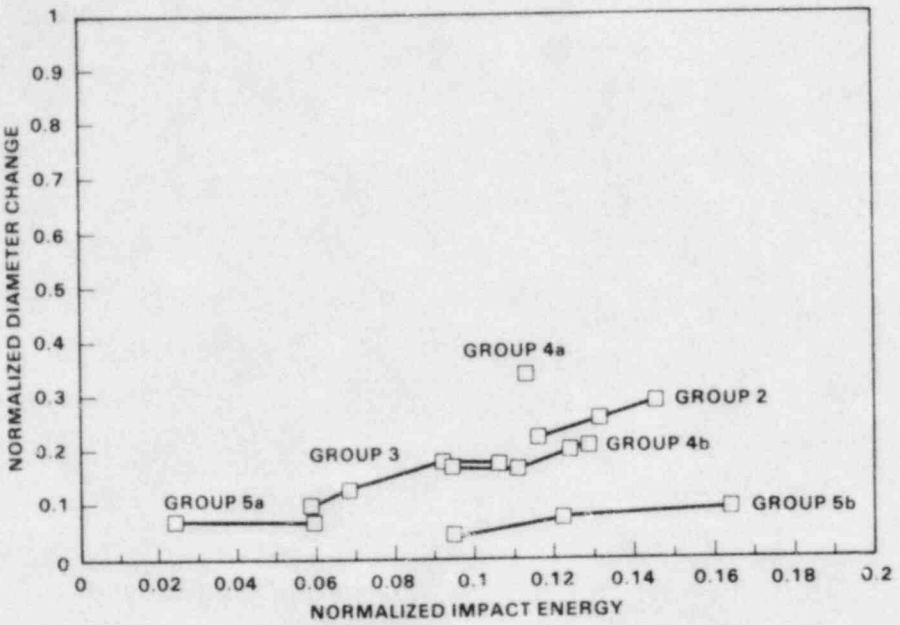

FIGURE 4. Normalized Diameter Change Data

FUTURE WORK

During the next quarter, completion of the hinge study and further development of the crack/bend model will be emphasized. The results of these tasks will be combined with the spacing distribution data so that the final test matrix can be finalized.

EVALUATION AND ACCEPTANCE OF WELDED AND WELD-REPAIRED STAINLESS STEEL FOR LWR SERVICE[a]

D. G. Atteridge, Project Manager

S. M. Bruemmer
B. Norton
R. E. Page

SUMMARY

Progress made during this quarter will be reported in NUREG/CR-3613.

INTRODUCTION

The objective of this Pacific Northwest Laboratory (PNL) program is to determine a method for evaluating the acceptance of welded and/or weld-repaired stainless steel (SS) piping for light-water reactor service. Based on experimental data, validated models will be developed for predicting the degree of sensitization and the intergranular stress corrosion cracking susceptibility in the heat-affected zone of SS weldments. The cumulative effects of material composition, past fabrication procedures, past service exposure, weldment thermomechanical history, and projected component life after repair will be considered.

(a) FIN: B2449; NRC Contact: J. Muscara.

SEVERE CORE DAMAGE SUBASSEMBLY PROCUREMENT PROGRAM

POWER BURST FACILITY SEVERE FUEL DAMAGE (SFD) TEST PROJECT[a]

R. L. Goodman, Program Manager

G. S. Allison
A. J. Anthony
L. R. Bunnell
N. C. Davis
L. L. King
L. J. Parchen
J. O. Vining
G. D. White

SUMMARY

The Pacific Northwest Laboratory (PNL)—Power Burst Facility (PBF) SFD 1-4 fuel bundle and insulated shroud assemblies were completed and delivered on schedule to the Idaho National Engineering Laboratory (INEL) on August 29, 1983. With this shipment, a total of five test train assemblies have been designed, developed, and fabricated by PNL and delivered to INEL in support of Phase 1 of the U.S. Nuclear Regulatory Commission (NRC)-sponsored PBF Severe Fuel Damage Program.

One metric ton of thorium dioxide powder has been received from Los Alamos National Laboratory. Extensive activity has been ongoing to investigate the processing characteristics of the thoria powder, using procedures developed in previous PNL work.

Long lead material and instrument components have been ordered for the fuel bundle, insulated shroud, and catch basket assemblies for the PBF Phase 2 SFD 2-1 and SFD 2-3 test assemblies. A large number of procurement commitments have been made, and some of the material and instrument components are now at PNL. The detailed design of the Phase 2 SFD 2-1 and SFD 2-3 fuel bundle, insulated shroud, and catch basket assemblies is continuing. The fuel bundle assembly and detailed drawings have been completed and are now being reviewed.

INTRODUCTION

The Severe Core Damage Subassembly Procurement Program includes the design, development of appropriate materials and supporting fabrication processes, and complete fabrication of fully instrumented test train assemblies for the NRC-sponsored test program at the PBF, Idaho Falls, Idaho. The objective of this PNL program is to study the behavior of light-water reactor fuel under severe high-temperature, flow-starvation conditions. In Phase 1, the peak cladding temperature will be limited to 2400K, which includes conditions ranging from those anticipated in a design-basis loss-of-coolant accident to those anticipated through the melting point of Zircaloy. Phase 2 tests will run to peak test assembly temperatures of 3100K, the melting temperature of UO_2. Many portions of the PBF Phase 1 and Phase 2 SFD tests should directly benefit the coolant boilaway and damage progression experiments in the National Research Universal (NRU) reactor due to similarities in the experimental objectives and for materials, instrumentation, and fabrication development.

FUTURE WORK

- Complete the detailed design of the Phase 2 SFD 2-1 and SFD 2-3 test assemblies.
- Continue thoria crucible development program in support of the Phase 2 tests to temperatures of 3100K.

(a) FINs: B2084, B2456, and B2864; NRC Contact: R. Van Houten.

ESSOR FUEL DAMAGE TEST PROGRAM SUPPORT[a]

F. E. Panisko, Project Manager
J. W. Upton, ESSOR Site Representative

SUMMARY

The U.S. Nuclear Regulatory Commission (NRC) site representative at Ispra, Italy, provided liaison and safety analysis support. Plans were made for the return of the site representative to the United States.

INTRODUCTION

The Super Sara Test Program (SSTP) was a major European Community effort to study reactor safety during rapid or large-break and slow or small-break loss-of-coolant accidents. The program was to be conducted in the SUPER SARA high-temperature, high-pressure loop in the ESSOR reactor, Ispra, Italy. The objective of the SSTP was to obtain experimental data on fuel rod deformation and postaccident coolability of damaged fuel assemblies after a loss-of-coolant-type accident. The testing program included loop construction and 21 in-reactor experiments simulating 7 large- and 12 small-break conditions in commercial pressurized and boiling water reactors. Funding for the SSTP was terminated by the European Council of Ministers.

FUTURE WORK

This project ended at the end of fiscal 1983. The site representative returned to the United States at the end of this quarter. No further work is planned.

(a) FIN: B2372-1; NRC Contact: R. Van Houten.

SEVERE CORE DAMAGE MATERIALS PROPERTY TESTS[a]

E. L. Courtright, Project Manager

L. R. Bunnell
J. E. Garnier
C. W. Griffin
J. T. Prater

SUMMARY

During this quarter, isothermal oxidation measurements were performed on Zircaloy in steam at 1600 to 1800°C. Viscosity measurements were conducted on zirconium with 5 to 10 mol% UO_2 at temperatures up to 2000°C

INTRODUCTION

The objective of this Pacific Northwest Laboratory (PNL) program is to perform high-temperature materials property tests and to provide data that will assist in the planning and analysis of U.S. Nuclear Regulatory Commission (NRC) severe core damage fuel behavior irradiation tests. High-temperature (>1600°C) ex-reactor physical property data and reactor kinetics data are needed on cladding and cladding/fuel/structure reaction products to model rod oxidation behavior and to properly account for the melting and refreezing of the cladding. Zircaloy/H_2O/UO_2 reaction kinetics will be studied, and the viscosities of liquefied fuel for several Zr/UO_2 compositions will be determined.

TECHNICAL PROGRESS

Kinetic studies of Zircaloy/steam reactions were conducted at 1600 to 1800°C in a flowing steam environment. The specimens were heated from the back side using a laser. A two-color infrared pyrometer monitored the temperature of the front side of the sample and controlled the laser power. To achieve isothermal conditions, the specimens were heated to a predetermined temperature plateau in argon and then steam was introduced through a fast-acting valve. The ensuing oxidation resulted in a rapid rise to the desired temperature, which was then held constant by controlling the laser heat input.

Each test was terminated after various time increments by shutting off the steam and laser power while introducing a rapid quench with argon gas. Isothermal temperature control of ±7°C at 1600°C, ±10°C at 1690°C, and ±18°C at 1780°C was achieved. The small amount of oxidation that occurred during the initial exothermic reaction to temperature was measured independently and subtracted to provide true isothermal growth kinetics.

Metallographic sectioning of the samples indicated that oxide growth on the front surface was very uniform. The growth kinetics of the oxide layer was parabolic. The study confirmed the previous findings of Urbanic that found a discontinuity in the oxide growth rate at 1580°C coinciding with the tetragonal-to-cubic phase transformation in ZrO_2.

(a) FINs: B2455; NRC Contact: R. Van Houten

Viscosity measurements to 2000°C were performed on Zr/UO_2 mixtures containing 5, 7.5, and 10 mol% UO_2. An oscillating cup viscometer was used, and the molten material was contained in ThO_2 crucibles. Although this crucible material was not entirely free of reaction with the sample, it was better than any other known substance. Decay constants were measured experimentally at several temperatures and these were then used to calculate the viscosity. Pure zirconium melted near 1850°C, and its viscosity rapidly dropped to a constant value of 3 centipoise above 1925°C. Mixtures of Zr with 5, 7.5, and 10 mol% UO_2 appeared to melt near 1950°C. At 2000°C, the mixture was still highly viscous, suggesting that the mixture still contained a solid phase. Recent German work by Skokan et al.[1] has confirmed that these mixtures should not have been a single liquid phase at 2000°C. These results are in contradiction with the earlier work by Politis.[2]

FUTURE WORK

- Kinetic studies of the Zircaloy reaction in Ar/H_2O and H_2/H_2O environments will be initiated.
- Laser Raman spectroscopy will be added to the oxidation experiment to study H_2 blanketing.
- The oxidation kinetics of molten Zircaloy in steam will be determined.
- The viscosity of Zr/UO_2 mixtures will be measured at higher temperatures and at greater UO_2 concentrations.
- The extent of reaction of ThO_2 crucibles with molten Zr/UO_2 mixtures will be determined, and its effect on the viscosity measurement will be established.

REFERENCES

1. Skokan, A., et al. 1983. "Investigation of the Phase Equilibria in the Ternary System U-Zr-O." KFK-3350, PNS Jahresbericht, Federal Republic of Germany.
2. Politis, C. 1975. "Investigation of the Ternary Uranium-Zirconium-Oxygen System." KFK-2167, Federal Republic of Germany.

COBRA APPLICATIONS(a)

M. J. Thurgood, Project Manager

T. E. Guidotti
J. M. Kelly

SUMMARY

The COBRA/TRAC computer code was used to simulate a one-dimensional (1-D) analysis of a large-break loss-of-coolant accident (LOCA) in a pressurized water reactor (PWR). The predicted peak cladding temperatures compared closely to a TRAC-PF1 prediction. COBRA-TF was used to predict reflood tests from the FLECHT-SEASET 21-rod unblocked bundle and the FEBA 5 x 5 grid effects tests.

INTRODUCTION

The COBRA computer code is being developed for the U.S. Nuclear Regulatory Commission (NRC) to provide better digital computer codes for assessing the behavior of full-scale reactor systems under postulated accident conditions. This Pacific Northwest Laboratory (PNL) project has three main objectives:

- to develop a water reactor primary system simulation capability that can model complex internal vessel geometries such as those encountered in upper head injection (UHI)-equipped PWRs
- to develop a hot bundle/hot channel analysis capability to evaluate the thermal-hydraulic performance of light-water reactor (LWR) fuel bundles during postulated accidents
- to develop a containment code capable of simulating the steam water blowdown and hydrogen distribution phases of an accident.

The resulting codes—COBRA/TRAC, COBRA-TF, and COBRA-NC—are being used to perform pre- and post-test analysis of LWR components and system effects experiments.

COBRA-TF is formulated to model 3-D, two-phase flow using a three-field representation: the vapor field, the continuous liquid field, and the droplet field. The model allows thermal nonequilibrium between the liquid and vapor phases and allows each of the three fields to move at a different velocity. Thus, one can mechanistically treat a continuous liquid core or film moving at a low or possibly negative velocity from which liquid drops are stripped off and carried away by the vapor phase. This feature is essential in the treatment of the hydrodynamics encountered during the reflooding phase of a LOCA. The treatment of the droplet field is also essential in predicting other phenomena such as countercurrent flow limiting (CCFL), upper plenum deentrainment and fallback, and two-phase jet impingement.

The code features flexixble noding, which allows modeling of such complex geometries as slotted control rod guide tubes, jet pumps, and core bypass regions. These geometries cannot be easily modeled in regular Cartesian or cylindrical mesh coordinates; however, since they have significant impact on the thermal-hydraulic response of the system, these geometries must be modeled with reasonable accuracy.

(a) FIN: B2041; NRC Contacts: J. T. Han and T. Lee.

The fuel rod heat transfer model uses a rezoning mesh to reduce the rod heat transfer mesh size automatically in regions of high heat flux or steep temperature gradients and to increase the mesh size in regions of low heat flux. This model has proven very effective in resolving the boiling curve in the region of the quench front.

TECHNICAL PROGRESS

COBRA/TRAC APPLICATIONS

A COBRA/TRAC large-break LOCA simulation in a non-UHI PWR was completed. The input model was developed from the same information that Los Alamos National Laboratory (LANL) used to create an input deck for an equivalent TRAC-PF1 calculation. Both calculations were intended to be best-estimate predictions with one main difference: the 1-D COBRA/TRAC mesh consisted of 60 cells in the vessel while the 3-D TRAC-PF1 mesh consisted of 544 cells in the vessel. The purpose of this simulation was to compare COBRA/TRAC with TRAC-PF1 and to verify the best-estimate models and input used in the TRAC-PF1 calculation.

Peak cladding surface temperatures for the two calculations are compared in Figure 1. The TRAC-PF1 mesh used cylindrical coordinates in the vessel and, in this case, had two radial rings in the core. Both calculations (Figure 1a) predicted that the center of the core would quench during blowdown. The quench was caused by water from the upper head as it flowed down the guide tubes and entered the core. The peak temperature in the outside radial ring is shown in Figure 1b; the outside of the core did not quench until bottom reflood. According to LANL, the reduced heat transfer in this outer ring from 15 to 20 s occurred because of a lower mass flux in the outside than in the center of the core. TRAC-PF1 calculated a peak temperature of 995°F at 2.5 s; the COBRA/TRAC prediction was 1058°F at 5.0 s.

Although the peak temperatures are comparable, there are some major differences between the calculations. First, the temperature increase during the nearly adiabatic heatup phase from 0 to 2 s is steeper for TRAC-PF1 because LANL used a lower gap conductance value. Although it is difficult to get a clear-cut answer for best-estimate versus evaluation-model values of gap conductance, it appears that the LANL value is too low for a best-estimate analysis where middle-of-life fuel is assumed. Values used by COBRA/TRAC were calculated from a dynamic gap conductance model that was assessed against FRAPCON-2, a best-estimate fuel rod code.(1)

A second difference is in the predicted effect of continued pump operation. TRAC-PF1 predicted that a significant amount of water will enter the core due to the pump. COBRA/TRAC did not predict that behavior at all as indicated in Figure 2, a plot of the collapsed liquid level in the core. TRAC-PF1 refilled the core with as much as 10.8 ft of liquid at 6 s; in the COBRA/TRAC calculation, liquid from the pumps flowed out the broken cold leg and not into the core.

The exact cause of this discrepancy has not been established. It seems to be related to the break flow rates. The total mass discharged from the break was lower for TRAC-PF1 as can be seen in Figure 3 by comparing upper plenum pressures. After 3 s, the pressure was higher in TRAC-PF1 than in COBRA/TRAC, indicating that less mass had been discharged. This slower blowdown allowed the pumped liquid to remain in the vessel and forced liquid through the core instead of flowing out the break. It should be noted that recent comparisons with calculations performed by Westinghouse verify the pressures predicted by COBRA/TRAC.

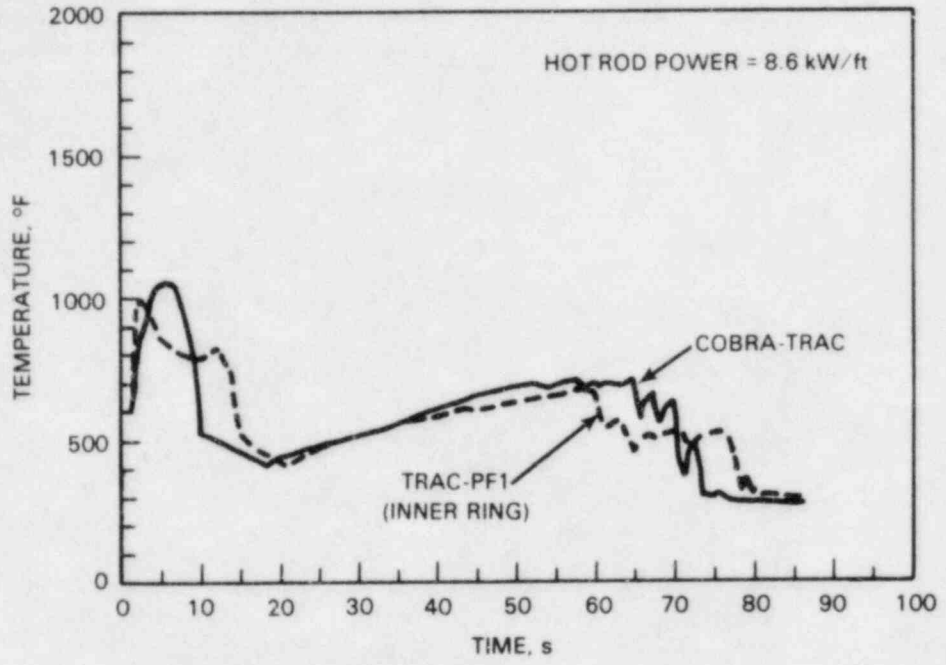

(a) COBRA-TRAC and Inner Ring of TRAC-PF1

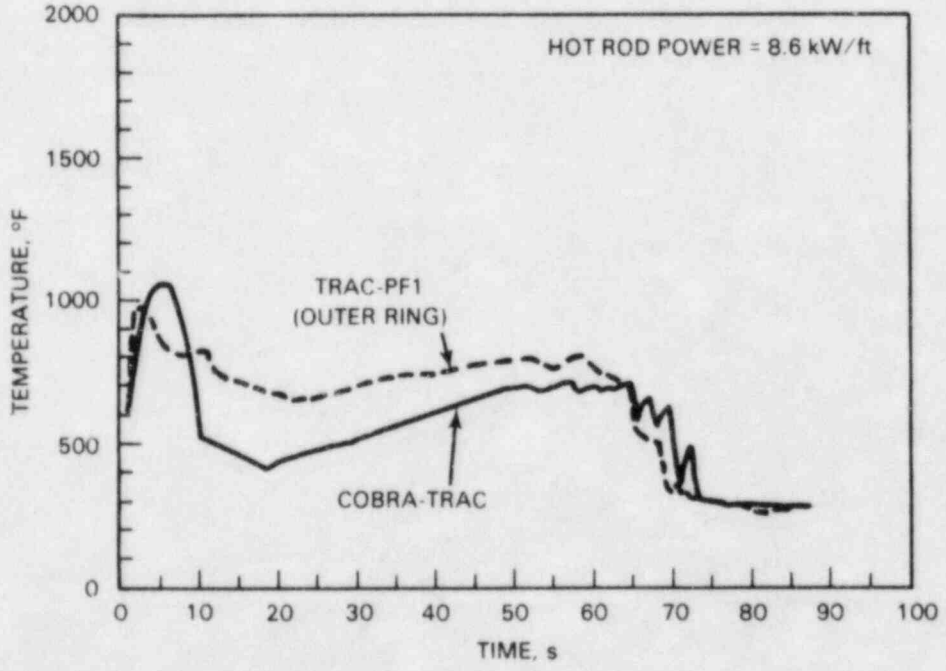

(b) COBRA-TRAC and Outer Ring of TRAC-PF1

FIGURE 1. Peak Cladding Surface Temperatures Predicted by COBRA-TRAC and TRAC-PF1

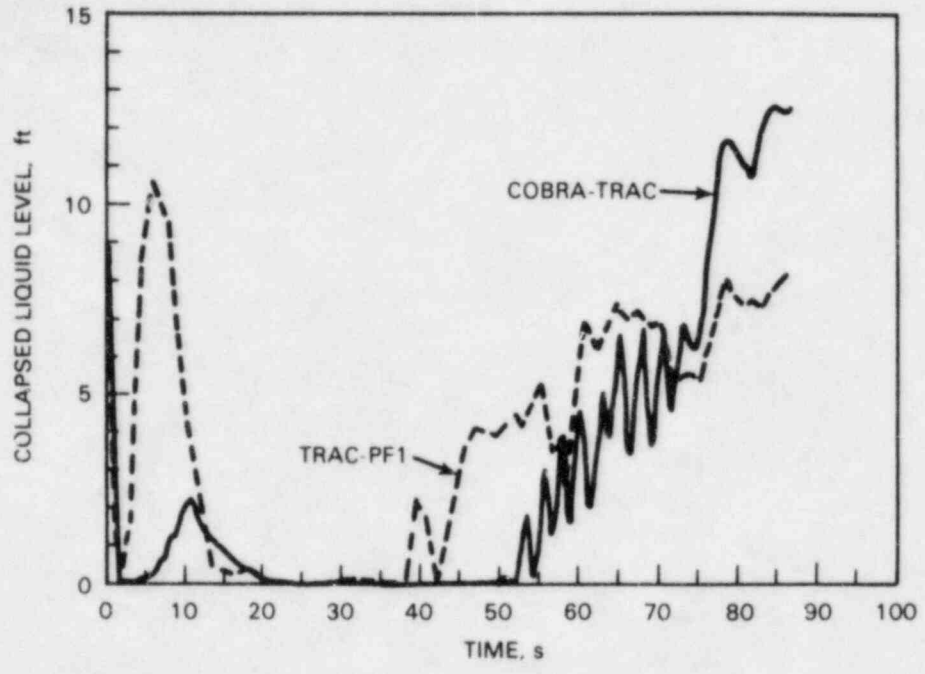

FIGURE 2. Collapsed Liquid Level Versus Time for COBRA-TRAC and TRAC-PF1

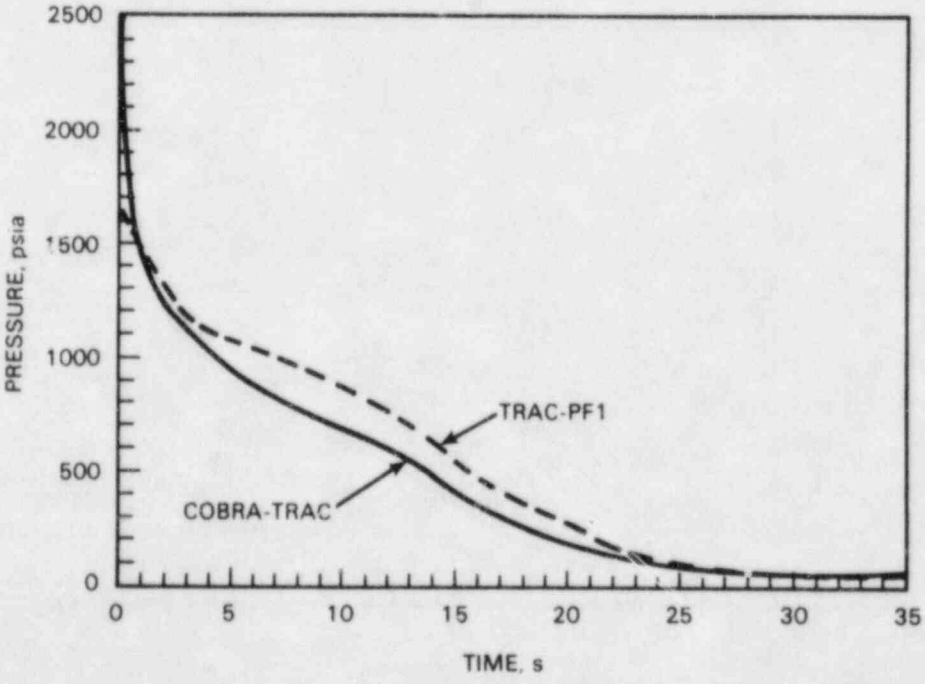

FIGURE 3. Upper Plenum Pressure Versus Time for COBRA-TRAC and TRAC-PF1

HOT BUNDLE CODE DEVELOPMENT

A joint project is being conducted with the FLECHT-SEASET program to address Appendix K steam cooling/flow blockage rules. The first task of the project is to modify COBRA-TF to accurately predict reflood tests with low flooding rates and high temperatures. Reflood tests for the FLECHT-SEASET 21-rod unblocked bundle and FEBA 5 x 5 grid effects tests are compared below. The test conditions were:

Parameter	FLECHT-SEASET Test 43208A	FEBA Run 216
Pressure, psia	40.6	60
Flooding rate, in./s	1.50	1.50
Peak power, kW/ft	0.70	0.80
Initial rod temperature, °F	1604	1479

The quench front location as a function of time for Test 43208A is shown in Figure 4. Predicted heater rod surface temperatures are compared with rod temperature histories at 72 in. and 96 in. in Figure 5. Although the 72-in. elevation is well predicted by COBRA-TF, a significant variation between the calculated and measured data occurs at the 96-in. elevation after turnaround time. Since the 96-in. elevation was well predicted for a similar test (31203) in the 161-rod bundle, it is believed this discrepancy is due to some phenomena peculiar to the 21-rod bundle that is not being modeled adequately. Possible candidates include:

- thermal radiation to the housing
- low water inventory due to inaccurate prediction of housing quench
- excessive grid effect at the 83-in. grid spacer.

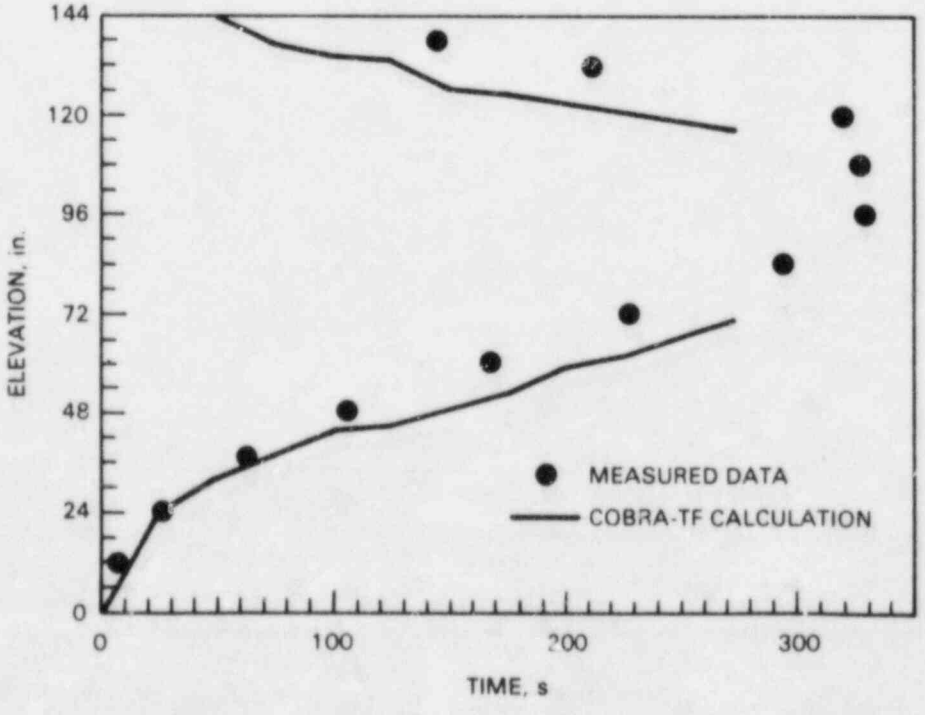

FIGURE 4. Quench Front Elevation Versus Time for FLECHT-SEASET Test 43208A

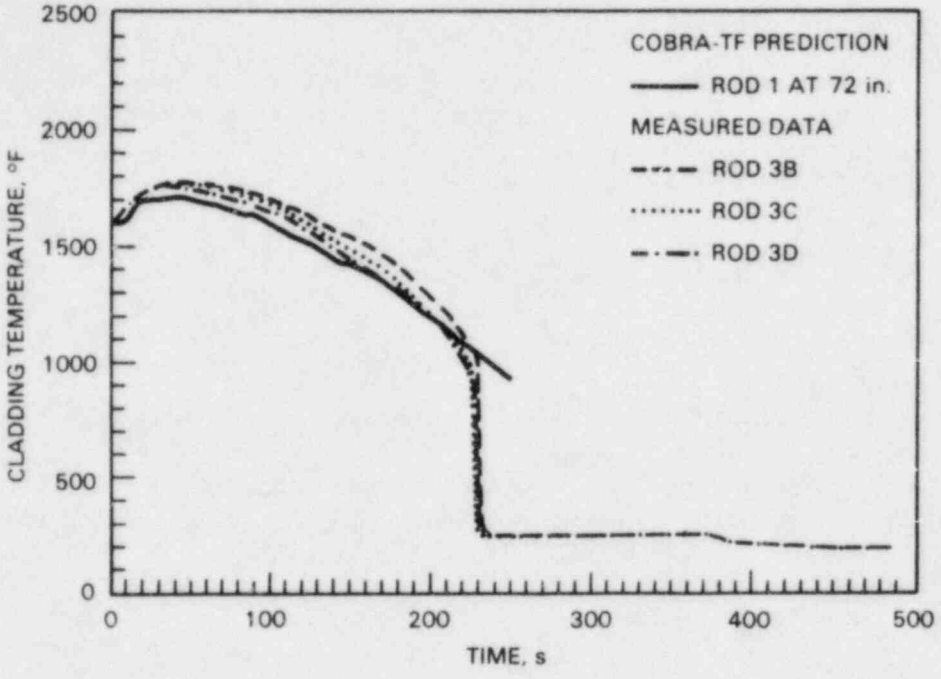

(a) 72-in. Elevation

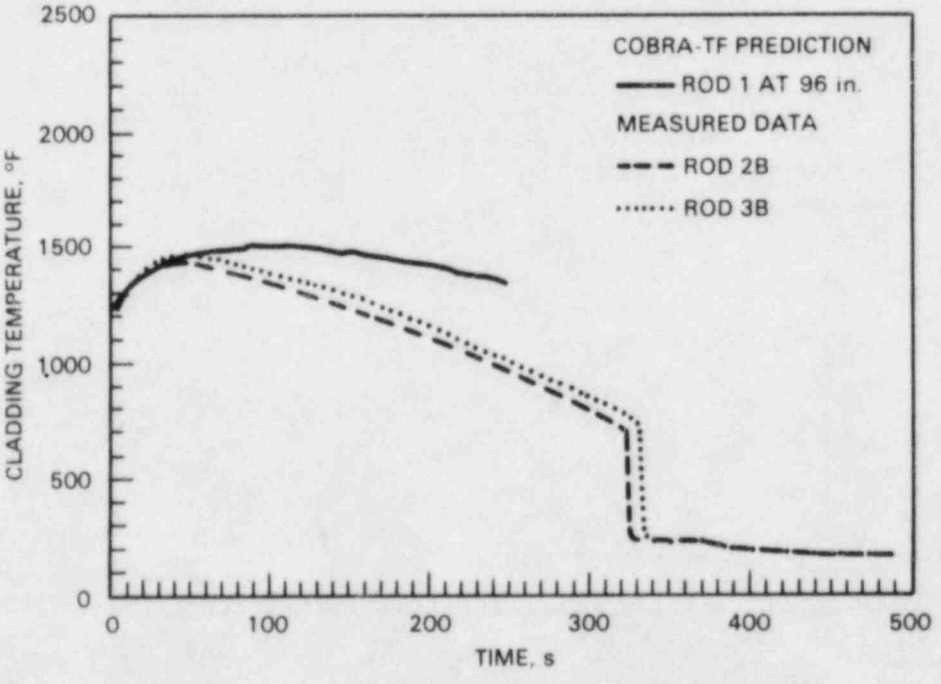

(b) 96-in. Elevation

FIGURE 5. Predicted and Measured Cladding Temperatures Versus Time at 72-in. and 96-in. Elevations

To eliminate the uncertainty associated with predicting the housing temperature and quench behavior, a housing boundary condition model was implemented. Experimental data were used to set housing temperatures and quenching heat release rates during a COBRA-TF transient calculation. Several bundle heatup transients will be simulated to test the thermal radiation model.

Predicted and measured quench behaviors are compared in Figure 6 for FEBA Run 216; measured and calculated rod temperature histories 100 mm downstream from the midplane spacer grid are shown in Figure 7. Both the quench and rod temperature behavior are well predicted. The heat transfer benefit derived from a spacer grid is illustrated in Figure 8. Run 216 includes the grid spacer at 1950 mm and Run 229 does not. An approximately 100°F temperature drop occurs immediately downstream from the grid and a 45°F temperature decrease occurs just prior to the next grid. The COBRA-TF calculation, which used 8-in. axial nodes in the grid region, predicted the enhanced heat transfer downstream from a spacer grid reasonably well.

COBRA-NC CONTAINMENT APPLICATIONS

The COBRA-NC Users' Manual and the assessment report were completed and will be submitted for NRC publication.

FUTURE WORK

During the next quarter, efforts will be made to resolve the difficulties with the 21-rod bundle simulations. Flow blockage models will be installed and debugged so that the blocked bundle simulations can begin as soon as the 21-rod unblocked simulations are satisfactory. Application of COBRA-NC to pre- and post-test results will continue, and COBRA/TRAC will continue to be assessed against new data.

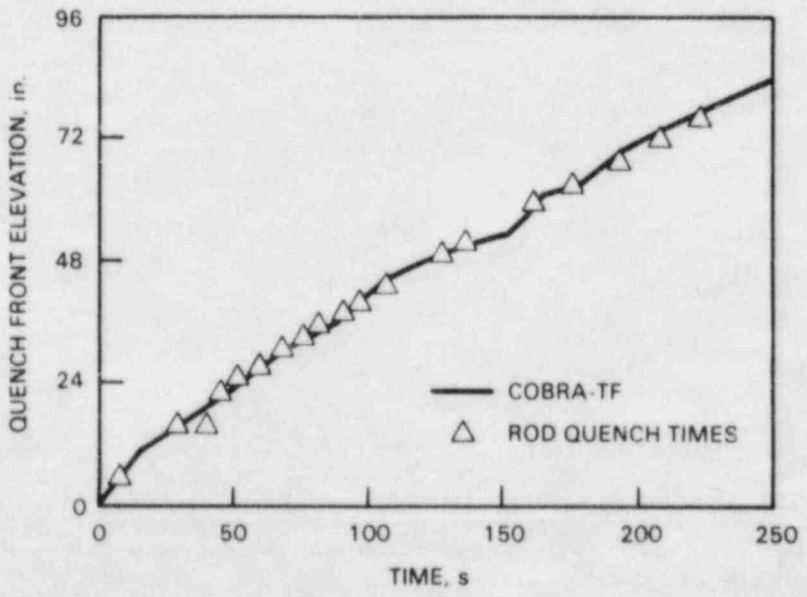

FIGURE 6. Predicted and Measured Quench Front Elevations Versus Time

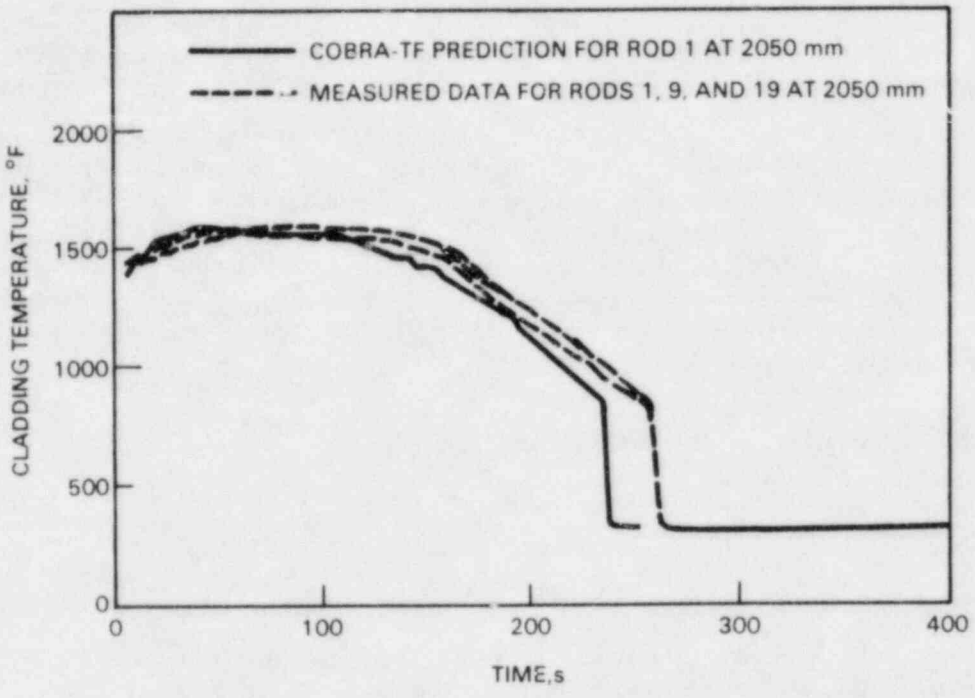

FIGURE 7. Predicted and Measured Cladding Temperatures Versus Time

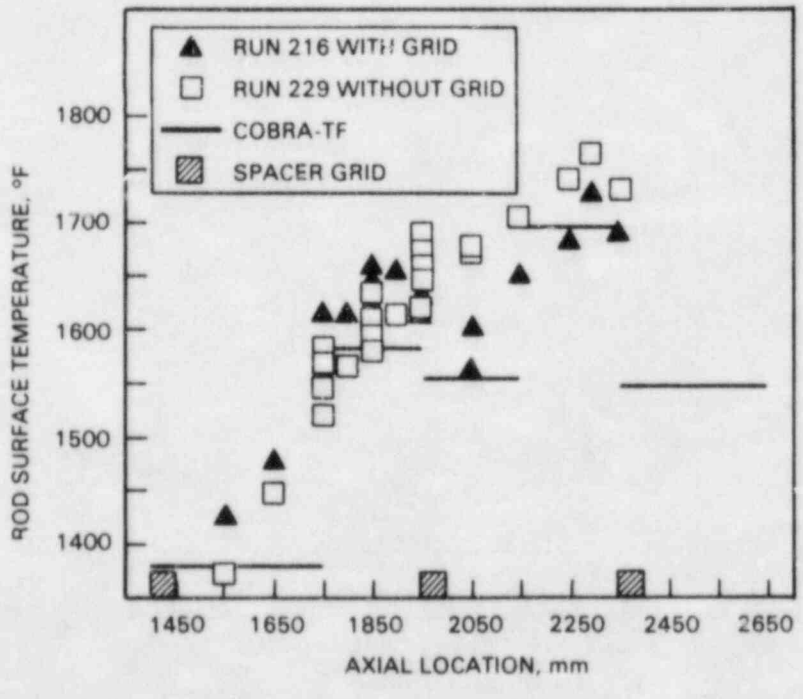

FIGURE 8. Spacer Grid Effects

REFERENCES

1. Berna, G. A., et al. 1981. *FRAPCON-2: A Computer Code for the Calculation of Steady-State Thermal-Mechanical Behavior of Oxide Fuel Rods.* NUREG/CR-1845, Idaho National Engineering Laboratory, Idaho Falls, Idaho.

COOLANT BOILAWAY AND DAMAGE PROGRESSION EXPERIMENTS IN THE NRU REACTOR[a]

F. E. Panisko, Program Manager
J. P. Pilger, Deputy Project Manager

SUMMARY

Work is progressing on the design, procurement, and safety analyses associated with the first full-length high-temperature (FLHT-1) severe fuel damage (SFD) experiment to be performed in the National Research Universal (NRU) reactor. This experiment was scheduled for May 1984; however, the test may be delayed due to current financial constraints. The design of the high-temperature shroud, including instrumentation layout and fuel rods, was completed. Design of the complete test train including loop modifications and test effluent control monitor (ECM) continued during this quarter. Long lead time purchase orders were placed. The preliminary safety analysis report (PSAR) was completed and issued to staff at Chalk River Nuclear Laboratory (CRNL).

INTRODUCTION

Two FLHT experiments will be conducted to provide data for evaluating SFD progression behavior and fuel debris bed coolability under degraded core conditions. Pacific Northwest Laboratory (PNL) will conduct these experiments in the NRU reactor at Chalk River, Ontario. These experiments are the initial tests in the Coolant Boilaway and Damage Progression (CBDP) Program, which is sponsored by the U.S. Nuclear Regulatory Commission (NRC) in support of the SFD program.

The first experiment (FLHT-1) will provide data for investigating the full-length integral effects of a simulated pressurized water reactor (PWR) coolant boilaway accident with fuel rods reaching temperatures as high as 2150K (3400°F). The boilaway transient for FLHT-1 will be stabilized at several temperature levels by controlling the flow rate of the makeup coolant water in the assembly. Data such as coolant flow rate, coolant level rate of change, steam production, and hydrogen generation rate will be collected as a function of the increasing temperatures to help evaluate degraded core behavior.

The second experiment (FLHT-2) will simulate a PWR degraded core accident where the natural boilaway of the coolant will result in fuel temperatures up to 2480K (4000°F). Operating conditions and design requirements for FLHT-2 will be developed from information obtained during FLHT-1. The operating performance of high-temperature instrumentation, safety features, and the hydrogen measurement and steam/off-gas velocity measurement systems are of particular interest. FLHT-2 design features will be similar to those for FLHT-1 except that different shroud insulation and thermocouple sensors may be used for the higher temperature operation during continuous boilaway of the test assembly coolant.

Many of the test train design and fabrication features and testing methods developed as part of the loss-of-coolant accident (LOCA) program conducted in the NRU reactor will be used in the CBDP Program; for example, coolant water level measurement using time domain reflectometry, remote pressure sensing to detect fuel cladding failure times, a spray desuperheater to control outlet steam temperature, and the NRU loop facilities that provide thermal-hydraulic control of operating conditions. These capabilities along with the development of high-temperature instrumentation and a hydrogen measuring system will be used to evaluate the degraded core phenomena during the experiments.

(a) FIN: B2277; NRC Contact: R. Van Houten.

TECHNICAL PROGRESS

The objective of the CBDP experiments is to obtain integrated degraded core behavior information under prototypic LWR conditions. Work this quarter continued at a reduced pace consistent with available funding. One of the main accomplishments was the completion of the PSAR for the FLHT tests. The report was transmitted to CRNL for review and concurrence. Another active area this quarter was on the FLHT test assembly design. The insulated shroud and 12-rod FLHT bundle preliminary detail designs were completed. Conceptual designs of the ECM including the hydrogen measuring system continued to evolve during this quarter. An improved data acquisition and control system was received, and software development for its use will begin next quarter. Necessary modifications to the test loop for the FLHT tests were discussed at CRNL with the NRU staff.

FUTURE WORK

Near the end of this quarter, a program modification was made at the request of NRC. The current CBDP program now includes tests MT-6A and MT-6B, which will be conducted in June 1984. The FLHT-1 test will be conducted in November 1984. Work will begin or continue in all of the following areas to meet the MT-6A, MT-6B, and FLHT-1 test dates:

- test assembly design
- test train hardware development, fabrication, and assembly
- licensing for shipment to Canada
- thermal-hydraulic calculation for test operations and safety analyses
- neutronics analysis related to safety
- test assembly instrumentation design and procurement
- effluent control module, including H_2 measurement
- data acquisition and control logic development
- test safety analyses
- quality control and assurance
- loop modification at CRNL.

STEAM GENERATOR GROUP PROJECT[a]

R. A. Clark, Project Manager
M. Lewis, Assistant Project Manager

R. P. Allen
R. L. Bickford
A. S. Birks
P. G. Doctor
A. B. Johnson, Jr.
W. D. Reece
E. B. Schwenk
K. R. Wheeler

SUMMARY

Information on the Steam Generator Group Project will no longer be reported in this quarterly report. A separate quarterly report will be issued on project activities.

(a) FIN: B2097; NRC Contact: J. Muscara.

DISTRIBUTION

No. of Copies

OFFSITE

U.S. Nuclear Regulatory Commission
Division of Technical Information
and Document Control
7920 Norfolk Avenue
Bethesda, MD 20014

W. J. Collins
U.S. Nuclear Regulatory Commission
Office of Inspection and Enforcement
Washington, DC 20555

R. B. Foulds
U.S. Nuclear Regulatory Commission
Office of Nuclear Regulatory Research
1130-SS
Washington, DC 20555

J. T. Han
U.S. Nuclear Regulatory Commission
Office of Nuclear Regulatory Research
1130-SS
Washington, DC 20555

W. Hazelton
U.S. Nuclear Regulatory Commission
Office of Nuclear Reactor Regulation
Washington, DC 20555

M. Hum
U.S. Nuclear Regulatory Commission
Office of Nuclear Reactor Regulation
Washington, DC 20555

Y. Hsii
U.S. Nuclear Regulatory Commission
Division of Systems Integration
Office of Nuclear Reactor Regulation
Washington, DC 20555

T. Lee
U.S. Nuclear Regulatory Commission
Office of Nuclear Regulatory Research
1130-SS
Washington, DC 20555

G. P. Marino
U.S. Nuclear Regulatory Commission
Office of Nuclear Regulatory Research
1130-SS
Washington, DC 20555

10 J. Muscara
U.S. Nuclear Regulatory Commission
Office of Nuclear Regulatory Research
1130-SS
Washington, DC 20555

No. of Copies

H. H. Scott
U.S. Nuclear Regulatory Commission
Office of Nuclear Regulatory Research
1130-SS
Washington, DC 20555

L. Shotkin
U.S. Nuclear Regulatory Commission
Office of Nuclear Regulatory Research
1130-SS
Washington, DC 20555

M. Vagins
U.S. Nuclear Regulatory Commission
Office of Nuclear Regulatory Research
1130-SS
Washington, DC 20555

R. Van Houten
U.S. Nuclear Regulatory Commission
Office of Nuclear Regulatory Research
1130-SS
Washington, DC 20555

G. Weidenhamer
U.S. Nuclear Regulatory Commission
Office of Nuclear Regulatory Research
1130-SS
Washington, DC 20555

E. O. Woolridge
U.S. Nuclear Regulatory Commission
Office of Nuclear Regulatory Research
1130-SS
Washington, DC 20555

F. Shakir
Department of Metallurgy
Association of American Railroads
3140 S. Federal
Chicago, IL 60616

L. J. Anderson, B2402
Dow Chemical Company
Texas Division
P.O. Drawer K
Freeport, TX 77541

L. Agee
Electric Power Research Institute
P.O. Box 10412
Palo Alto, CA 94304

J. Mundis
Electric Power Research Institute
P.O. Box 10412
Palo Alto, CA 94304

No. of Copies

B. R. Sehgal
Electric Power Research Institute
P.O. Box 10412
Palo Alto, CA 94304

SM-ALC/MMET
Attn: Capt. J. Rodgers
McClellan AFB, CA 95652

W. L. Pearl
NWT Corporation
7015 Realm Drive
San Jose, CA 95119

W. P. Eatherly
Union Carbide Company
Oak Ridge National Laboratory
P. O. Box X
Oak Ridge, TN 37830

J. Whittaker
Union Carbide Company
Oak Ridge National Laboratory
Oak Ridge, TN 37830

M. C. Jon
Western Electric, ERC
P. O. Box 900
Princeton, NJ 08540

J. Vahaviolos
Western Electric, ERC
P. O. Box 900
Princeton, NJ 08540

FOREIGN

D. Birchon
Admiralty Materials Laboratory
Holton Health Poole
Dorset, U.K.

A.C.E. Sinclair
Research Division
Berkeley Nuclear Laboratories
Berkeley
Gloucestershire, GL 13 9 PB
U.K.

W. G. Cunliffe
Building 396
British Nuclear Fuels Ltd.
Springfields Works
Salwick, Preston
Lances. PR40XJ
U.K.

No. of Copies

ONSITE

50 **Pacific Northwest Laboratory**

J. M. Alzheimer
D. G. Atteridge
M.C.C. Bampton
J. O. Barner
R. A. Clark
E. L. Courtright
M. E. Cunningham
R. L. Dillon
S. R. Doctor
S. K. Edler (3)
M. D. Freshley
J. E. Garnier
R. L. Goodman
T. E. Guidotti
C. R. Hann
P. G. Heasler
P. H. Hutton
J. M. Kelly
R. J. Kurtz
D. D. Lanning
R. P. Marshall
J. L. McElroy
W. C. Morgan
F. E. Panisko
L. T. Pedersen
J. P. Pilger
G. J. Posakony
J. T. Prater
W. N. Rausch
G. E. Russcher
E. B. Schwenk
E. P. Simonen
F. A. Simonen
J. R. Skorpik
A. M. Sutey
T. T. Taylor
M. J. Thurgood
G. L. Tingey
D. S. Trent
C. L. Wheeler
R. E. Williford
Technical Information (5)
Publishing Coordination (2)

NRC FORM 335 (11-81)

U.S. NUCLEAR REGULATORY COMMISSION

BIBLIOGRAPHIC DATA SHEET

1. REPORT NUMBER (Assigned by DDC)
NUREG/CR-3307, Vol. 3
PNL-4706-3

4. TITLE AND SUBTITLE (Add Volume No., if appropriate)
Reactor Safety Research Programs
Quarterly Report
July-September 1983

2. (Leave blank)

3. RECIPIENT'S ACCESSION NO.

7. AUTHOR(S)
S. K. Edler, ed.

5. DATE REPORT COMPLETED
MONTH March YEAR 1984

9. PERFORMING ORGANIZATION NAME AND MAILING ADDRESS (Include Zip Code)
Pacific Northwest Laboratory
P.O. Box 999
Richland, WA 99352

DATE REPORT ISSUED
MONTH April YEAR 1984

6. (Leave blank)

8. (Leave blank)

12. SPONSORING ORGANIZATION NAME AND MAILING ADDRESS (Include Zip Code)
Division of Accident Evaluation
Division of Engineering Technology
Office of Nuclear Regulatory Research
U.S. Nuclear Regulatory Commission
Washington, DC 20555

10. PROJECT/TASK/WORK UNIT NO.

11. FIN NO.
B2452, B2383, B2449, B2101, B2088, B2289, B2043, B2084, B2456, B2864, B2372, B2455, B2041, B2277, B2097

13. TYPE OF REPORT
Quarterly

PERIOD COVERED (Inclusive dates)
July-September 1983

15. SUPPLEMENTARY NOTES

14. (Leave blank)

16. ABSTRACT (200 words or less)

ABSTRACT

This document summarizes work performed by Pacific Northwest Laboratory from July 1 through September 30, 1983, for the Division of Accident Evaluation and the Division of Engineering Technology, U.S. Nuclear Regulatory Commission. Evaluations of nondestructive examination (NDE) techniques and instrumentation include demonstrating the feasibility of determining the strength of structural graphite, evaluating the feasibility of detecting and analyzing flaw growth in reactor pressure boundary systems, and examining NDE reliability and probabilistic fracture mechanics. Accelerated pellet-cladding interaction modeling is being conducted to predict the probability of fuel rod failure under normal operating conditions. Experimental data and analytical models are being provided to aid in decision making regarding pipe-to-pipe impacts following postulated breaks in high-energy fluid system piping. Experimental data and validated models are being used to determine a method for evaluating the acceptance of welded or weld-repaired stainless steel piping. Thermal-hydraulic models are being developed to provide better digital codes to compute the behavior of full-scale reactor systems under postulated accident conditions. High-temperature materials property tests are being conducted to provide data on severe core damage fuel behavior. Severe fuel damage accident tests are being conducted at the NRU reactor, Chalk River, Canada; and an instrumented fuel assembly irradiation program is being performed at Halden, Norway. Fuel assemblies and analytical support are being provided for experimental programs at other facilities, including the Super Sara Test Program, Ispra, Italy, and experimental programs at the Power Burst Facility, Idaho National Engineering Laboratory, Idaho Falls, Idaho.

17. KEY WORDS AND DOCUMENT ANALYSIS
quarterly progress
severe fuel damage
FRAPCON computer code
fracture mechanics
COBRA applications
pellet-cladding interaction
thermal modeling

17a. DESCRIPTORS
nondestructive examination
in-service inspection
postirradiation examination
in-reactor testing
pipe-to-pipe testing

17b. IDENTIFIERS/OPEN-ENDED TERMS

18. AVAILABILITY STATEMENT
Unlimited

19. SECURITY CLASS (This report)
unclassified

21. NO. OF PAGES

20. SECURITY CLASS (This page)
unclassified

22. PRICE
$

NRC FORM 335 (11-81)

NUREG/CR-3307, Vol. 3
REACTOR SAFETY RESEARCH PROGRAMS QUARTERLY REPORT
JULY-SEPTEMBER 1983
APRIL 1984